



**NTNU – Trondheim**  
Norwegian University of  
Science and Technology

# Analysis of CO<sub>2</sub> heat pump for low energy residential building

**Aleksander Olsen Thoreby**

Master of Energy and Environmental Engineering

Submission date: June 2013

Supervisor: Natasa Nord, EPT

Norwegian University of Science and Technology  
Department of Energy and Process Engineering



EPT-M-2013-115

**MASTER THESIS**

for

Aleksander Olsen Thoreby

Spring 2013

Analysis of CO<sub>2</sub> heat pump for low energy residential building*Analyse av CO<sub>2</sub> varmepumpe til lavenergibolig***Background and objective**

Low-energy buildings require application of energy-efficient technologies like high quality building insulation, energy-efficient building services, and high level of heat recovery. The application of these technologies has led to changes in building energy demand. CO<sub>2</sub> heat pump has the property that the condenser heat is transferred at different temperature levels, high, medium, and low. Thus, the heat pump generates condenser heat at similar temperature level as the building requirements are, the high temperature heat for the domestic hot water, heat at mean temperature for the space heating, etc. Therefore, the CO<sub>2</sub> heat pump can be a very good solution for energy supply of low-energy houses. However, modelling of the CO<sub>2</sub> heat pump performance under operation can be challenging. Further, modelling the CO<sub>2</sub> heat pump performance and the building energy performance together can be very challenging. During the project assignment, the student developed simulation models of the building and the CO<sub>2</sub> heat pump in *EnergyPlus*. Some issues in the simulations have been identified.

This master thesis has aim to simulate operation of the CO<sub>2</sub> heat pump in a residential building. Parametric analysis and optimization of the CO<sub>2</sub> heat pump in a residential building should be performed. If necessary, different simulations programs could be implemented for the analysis. Data post-processing of the obtained results should be performed.

This project work is closely related to The Research Centre on Zero Emission Building at NTNU and SINTEF (FME ZEB) that has the vision to eliminate the greenhouse gas emissions caused by buildings. This national research center will place Norway in the forefront with respect to research, innovation and implementation within the field of energy efficient zero-emission buildings.

**The following tasks are to be considered:**

1. Literature review of the CO<sub>2</sub> heat pump technologies. The review should also include integration with storage system. Literature review of the building simulations.
2. Develop an energy supply system model that would include CO<sub>2</sub> heat pump and heat storages. Explain challenges in the modelling have to be explained. If necessary different modelling approaches could be included.

3. Analyse the developed model for different operation conditions. In order to find optimal operation parameters, a parametric study of the results could be performed.
4. Explain issues and challenges related to the modelling of the analysed system. Based on the results, define performance requirements for the analyzed CO<sub>2</sub> heat pump in the residential building.

-- ” --

Within 14 days of receiving the written text on the master thesis, the candidate shall submit a research plan for his project to the department.

When the thesis is evaluated, emphasis is put on processing of the results, and that they are presented in tabular and/or graphic form in a clear manner, and that they are analyzed carefully.

The thesis should be formulated as a research report with summary both in English and Norwegian, conclusion, literature references, table of contents etc. During the preparation of the text, the candidate should make an effort to produce a well-structured and easily readable report. In order to ease the evaluation of the thesis, it is important that the cross-references are correct. In the making of the report, strong emphasis should be placed on both a thorough discussion of the results and an orderly presentation.

The candidate is requested to initiate and keep close contact with his/her academic supervisor(s) throughout the working period. The candidate must follow the rules and regulations of NTNU as well as passive directions given by the Department of Energy and Process Engineering.

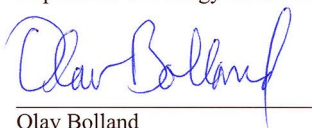
Risk assessment of the candidate's work shall be carried out according to the department's procedures. The risk assessment must be documented and included as part of the final report. Events related to the candidate's work adversely affecting the health, safety or security, must be documented and included as part of the final report.

Pursuant to “Regulations concerning the supplementary provisions to the technology study program/Master of Science” at NTNU §20, the Department reserves the permission to utilize all the results and data for teaching and research purposes as well as in future publications.

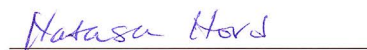
The final report is to be submitted digitally in DAIM. An executive summary of the thesis including title, student’s name, supervisor's name, year, department name, and NTNU's logo and name, shall be submitted to the department as a separate pdf file. Based on an agreement with the supervisor, the final report and other material and documents may be given to the supervisor in digital format.

- Work to be done in lab (Water power lab, Fluids engineering lab, Thermal engineering lab)  
 Field work

Department of Energy and Process Engineering, 9. February 2013



Olav Bolland  
Department Head



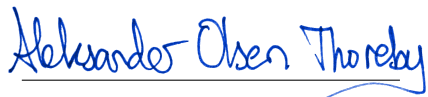
Natasa Nord  
Academic Supervisor

Research Advisor: Maria J. Alonso, SINTEF Energy Research

## Preface

This thesis is part of the final year in the Energy and Environmental Engineering program at NTNU. It makes up 30 credits for the 2013 spring term.

EnergyPlus, the software used for simulations in this project, had a very steep learning curve and both using the program and processing of the output data was time consuming. I would therefore like to thank my supervisor Natasa Nord in the Department of Energy and Process Engineering at NTNU not only for guidance during the writing of the thesis, but also for great help with the simulation software.



Aleksander Olsen Thoreby  
Trondheim, June 10, 2013



## Abstract

In low energy buildings heat loss is reduced through energy-saving measures like heat recovery of ventilation air and a well-insulated building envelope. Consequently the demand for domestic hot water often makes up a larger share of the annual heating demand than in traditional buildings. For this application heat pumps using CO<sub>2</sub> as a working fluid are seen as a promising alternative to conventional heat pumps. In the current study a transcritical CO<sub>2</sub> heat pump model for use in building simulations was developed. Some challenges related to the development and implementation of the model were pointed out.

A preliminary study of the model was performed in order to determine the optimal input parameters for the heat pump in the building of interest. The performance of the heat pump was analyzed over a range of operating conditions. Sizing recommendations for the main heat pump components were made, and a strategy for optimal control of the gas cooler pressure was presented.

The model was implemented into EnergyPlus and used for energy simulations of a low energy residential building consisting of three apartments. The heat pump performance was analyzed for different building usage patterns including "normal" use, increased demand for domestic hot water and night-time reduction of the indoor temperature. Simulation results showed an increase in overall system SPF from 2.51 to 2.64 in the case of increased domestic hot water demand because of more favorable operating conditions for the heat pump. Results further suggested that energy savings in the case of night-time temperature reduction would be minimal due to an increased demand for supplementary heating when reheating the building. In the latter case the overall system SPF was reduced to 2.43. Recommendations for achieving a better performance were made based on the simulations results.





## Sammendrag

I et lavenergibygg fører tiltak som varmegjenvinning av ventilasjonsluft og en godt isolert bygningskropp til et lavt varmetap. I en slik bolig utgjør derfor ofte oppvarming av tappevann en større andel av det totale oppvarmingsbehovet enn i tradisjonelle bygg. Varmepumper som benytter CO<sub>2</sub> som arbeidsmedium er antatt å være en god løsning i slike bygg. I denne oppgaven ble det utviklet en modell av en transkritisk CO<sub>2</sub>-varmepumpe. Noen utfordringer knyttet til utvikling og bruk av modellen ble påpekt.

En innledende studie av modellen ble utført under noen forenklende antakelser for å bestemme nødvendige inndata i videre simuleringer. Varmepumpens ytelse under varierende arbeidsbetingelser ble analysert, og strategi for optimal styring av gasskjølertrykket ble bestemt ut ifra dette. Det ble videre gitt anbefalinger om dimensjonering av varmepumpens hovedkomponenter.

Modellen ble implementert i programmet EnergyPlus og brukt i energisimuleringer av et lavenergi boligbygg bestående av tre leiligheter. Varmepumpens ytelse ble analysert ved forskjellige tilfeller av bruksmønstre for bygningen. Disse inkluderte "normal" bruk, økt varmtvannsbehov og nattsinking av innetemperaturen. Resultater indikerte en økning i systemets årsvarmefaktor fra 2.51 til 2.64 ved økt varmtvannsbehov på grunn av bedre arbeidsbetingelser for varmepumpen. Videre indikerte resultatene at det kan forventes en minimal energibesparelse ved å redusere innendørstemperaturen om natten grunnet et økt behov for tilleggsvarme ved gjenoppvarming av bygget. I sistnevnte tilfelle minket årsvarmefaktoren til 2.43. Anbefalinger for å oppnå forbedret ytelse ble gitt på grunnlag av simuleringsresultatene.



# Contents

<b>Abstract</b>	<b>i</b>
<b>Sammendrag</b>	<b>iii</b>
<b>1 Introduction</b>	<b>1</b>
1.1 Background . . . . .	1
1.2 Low energy buildings . . . . .	1
1.3 Objectives . . . . .	4
<b>2 CO<sub>2</sub> heat pump technology</b>	<b>5</b>
2.1 CO <sub>2</sub> as a refrigerant . . . . .	5
2.1.1 Properties of CO <sub>2</sub> . . . . .	5
2.1.2 The transcritical CO <sub>2</sub> heat pump cycle . . . . .	7
2.2 Heat pump design . . . . .	11
2.3 Integration with thermal storage and space heating systems	13
2.3.1 Domestic hot water . . . . .	17
2.3.2 Hydronic space heating . . . . .	19
2.4 System performance . . . . .	20
<b>3 Transcritical heat pump models in literature</b>	<b>23</b>
3.1 Brown and Domanski (2000) . . . . .	23
3.2 Stene (2004) . . . . .	24
3.3 Sarkar et al. (2006) . . . . .	25
3.4 Yokoyama et al. (2007) . . . . .	25
3.5 Cecchinato et al. (2011) . . . . .	26
3.6 Yamaguchi et al. (2011) . . . . .	27
3.7 Control of gas cooler pressure . . . . .	27
<b>4 Development of a transcritical heat pump model</b>	<b>29</b>
4.1 Heat pump model . . . . .	29
4.2 Implementation into EnergyPlus . . . . .	35
4.3 Preliminary study of model . . . . .	37
<b>5 Building and simulation inputs</b>	<b>43</b>
5.1 Building overview . . . . .	43
5.2 Domestic hot water and hydronic heating system . . . . .	45
5.3 Case study overview . . . . .	47

<b>6</b>	<b>Results</b>	<b>49</b>
6.1	Building peak load and energy consumption . . . . .	49
6.2	Initial comparison of energy use . . . . .	51
6.3	Case A: Base case . . . . .	53
6.4	Case B: Increased consumption of domestic hot water . .	55
6.5	Case C: Reduced indoor temperature during night-time .	57
<b>7</b>	<b>Conclusions and suggestions for further work</b>	<b>61</b>
	<b>References</b>	<b>63</b>
	<b>Computer software</b>	<b>67</b>
<b>APPENDICES</b>		
<b>A</b>	<b>List of digital attachments</b>	
<b>B</b>	<b>COP vs. gas cooler UA-value</b>	
<b>C</b>	<b>Optimal gas cooler pressure curves</b>	
<b>D</b>	<b>Heat pump model source code</b>	

## List of Figures

1.1	<i>Energy transformation</i> . . . . .	2
1.2	<i>Passive energy design pyramid</i> . . . . .	3
2.1	<i>Vapour pressure vs. temperature for selected refrigerants</i>	6
2.2	$\Delta T/\Delta p$ vs. temperature for selected refrigerants . . . . .	6
2.3	<i>The difference between a transcritical and subcritical cycle illustrated in a pressure-enthalpy diagram</i> . . . . .	8
2.4	Illustration of the average heat rejection temperature at small temperature glide in a temperature-enthalpy diagram	9
2.5	Illustration of the average heat rejection temperature at large temperature glide in a temperature-enthalpy diagram	10
2.6	<i>Specific heat of CO<sub>2</sub> as a function of temperature at supercritical pressures</i> . . . . .	10
2.7	<i>Principle of a transcritical heat pump</i> . . . . .	11
2.8	<i>Basic transcritical heat pump modified with a liquid receiver and a suction line heat exchanger (SLHX)</i> . . . . .	12
2.9	<i>Single gas cooler configuration</i> . . . . .	13
2.10	Single gas cooler connected to a storage tank . . . . .	14
2.11	Bipartite gas cooler in series configuration . . . . .	15
2.12	<i>Bipartite gas cooler in parallel configuration</i> . . . . .	15
2.13	<i>Tripartite gas cooler configuration</i> . . . . .	16
2.14	Internal gas cooler configurations . . . . .	17
2.15	DHW tank with a moving insulating plate separating the hot and cold water (Stene, 2004) . . . . .	18
2.16	<i>Relative energy savings as a function of SPF for a heat pump system covering 100%, 90% and 70% of annual demand, <math>\eta = 1</math>.</i> . . . . .	21
4.1	<i>The modeled heat pump process illustrated in a pressure-enthalpy chart</i> . . . . .	30
4.2	<i>Illustration of the gas cooler subsection division</i> . . . . .	32
4.3	<i>Illustration of one gas cooler subsection</i> . . . . .	32
4.4	Calculation steps for the heat pump model and the gas cooler model . . . . .	34
4.5	<i>Overview of the connections between the main HVAC simulation loops and half loops in the EnergyPlus systems manager (EnergyPlus, 2012)</i> . . . . .	35

4.6	<i>Illustration of the glycol mix loop on the evaporator side as modeled in EnergyPlus . . . . .</i>	36
4.7	<i>COP vs. gas cooler UA-value at different gas cooler pressures. Secondary fluid heated from 30 to 35°C, evaporator UA-value is 2000 W/K. . . . .</i>	39
4.8	<i>COP vs. gas cooler UA-value at different gas cooler pressures. Secondary fluid heated from 7 to 65°C, evaporator UA-value is 2000 W/K. . . . .</i>	39
4.9	<i>Comparison of the pressure predicted by Equation 4.13 and the actual optimal pressure in the range tested at constant outdoor temperature of 7°C. . . . .</i>	41
5.1	<i>Geometry and dimensions of the building used for simulations . . . . .</i>	44
5.2	<i>Floor plan of one apartment. All apartments had identical floor plans. . . . .</i>	44
5.3	<i>Illustration of EnergyPlus system . . . . .</i>	45
5.4	<i>Illustration of the DHW tank as modeled in EnergyPlus . . . . .</i>	46
6.1	<i>Monthly energy end-use for electric reference model . . . . .</i>	50
6.2	<i>Heating load duration curve for electric reference model . . . . .</i>	50
6.3	<i>Comparison of the total site energy consumption in each of the cases studied including space heating, DHW and el.specific use. . . . .</i>	52
6.4	<i>Comparison of the specific energy end-use distribution in each of the cases studied. . . . .</i>	52
6.5	<i>Comparison of heat pump coverage and supplementary system coverage of the heating demand in each of the cases studied. . . . .</i>	53
6.6	<i>Case A: Heating load duration curve . . . . .</i>	54
6.7	<i>Case A: Variation of COP with outdoor air temperature for the different heating modes. . . . .</i>	55
6.8	<i>Case B: Heating load duration curve . . . . .</i>	56
6.9	<i>Case B: Variation of COP with outdoor air temperature for the different heating modes. . . . .</i>	57
6.10	<i>Case A: Variation of first floor living room air temperature and heat pump heating load without night-time temperature reduction over the course of a typical winter day. . . . .</i>	58

6.11	<i>Case C: Variation of first floor living room air temperature and heat pump heating load with night-time temperature reduction over the course of a typical winter day. . . . .</i>	58
6.12	<i>Case C: Heating load duration curve . . . . .</i>	60
6.13	<i>Case C: Variation of COP with outdoor air temperature for the different heating modes. . . . .</i>	60
B.1	<i>COP vs. gas cooler UA-value at different gas cooler pressures. Secondary fluid heated from 30 to 35°C, evaporator UA-value is 400 W/K. . . . .</i>	70
B.2	<i>COP vs. gas cooler UA-value at different gas cooler pressures. Secondary fluid heated from 7 to 65°C, evaporator UA-value is 400 W/K. . . . .</i>	70
B.3	<i>COP vs. gas cooler UA-value at different gas cooler pressures. Secondary fluid heated from 30 to 35°C, evaporator UA-value is 700 W/K. . . . .</i>	71
B.4	<i>COP vs. gas cooler UA-value at different gas cooler pressures. Secondary fluid heated from 7 to 65°C, evaporator UA-value is 700 W/K. . . . .</i>	71
B.5	<i>COP vs. gas cooler UA-value at different gas cooler pressures. Secondary fluid heated from 30 to 35°C, evaporator UA-value is 1200 W/K. . . . .</i>	72
B.6	<i>COP vs. gas cooler UA-value at different gas cooler pressures. Secondary fluid heated from 7 to 65°C, evaporator UA-value is 1200 W/K. . . . .</i>	72
C.1	<i>Least-squares curve-fit of optimal gas cooler pressure variation with secondary fluid inlet temperature (Equation 4.13, Chapter 4.3) . . . . .</i>	73
C.2	<i>Least-squares curve-fit of optimal gas cooler pressure variation with secondary fluid setpoint temperature (Equation 4.13, Chapter 4.3) . . . . .</i>	73

## List of Tables

2.1	<i>Refrigerant properties (ASHRAE, 2005)</i> . . . . .	5
4.1	<i>Constant values assumed for parametric study of heat pump model</i> . . . . .	37
4.2	<i>Temperature ranges for which the optimal pressure was calculated</i> . . . . .	40
5.1	<i>Building envelope U-values [W/(m<sup>2</sup>-K)]</i> . . . . .	43
6.1	<i>Summary of simulation results for each case</i> . . . . .	59



# Nomenclature

## Symbols

A	Area	[m <sup>2</sup> ]
C	Heat capacity	[J/K]
c	Specific heat capacity	[J/(kg-K)]
E	Energy	[J], [kJ]
h	Specific enthalpy	[J/kg]
k	Correction factor	[-]
$\dot{m}$	Mass flow rate	[kg/s]
N	Number of subsections	[-]
NTU	Number of transfer units	[-]
P	Power	[W], [kW]
p	Pressure	[bar]
Q	Heat	[W], [kW]
T	Temperature	[°C], [K]
U	Overall heat transfer coefficient	[W/(m <sup>2</sup> -K)]
$\dot{V}$	Displacement rate	[m <sup>3</sup> /s]
W	Work	[W], [kW]

## Greek letters

$\rho$	Density	[kg/m <sup>3</sup> ]
$\eta$	Efficiency	[-]
$\lambda$	Heat pump coverage fraction	[-]
$\beta$	Heat loss factor	[-]
$\varepsilon$	Effectiveness	[-]

## Subscripts

C	Compressor
cr	Critical
D	Design
E	Evaporator
GC	Gas cooler
HP	Heat pump
in	Inlet condition
is	Isentropic
j	Subsection number
LZ	Lorentz
m	Mean
min	Minimum
opt	Optimal
out	Outlet condition
p	Constant pressure
r	Refrigerant
set	Setpoint
sf	Secondary fluid
SH	Superheat
v	Vapour
vol	Volumetric
w	Water

## Abbreviations

ACH	Air changes per hour
CFC	Chlorofluorocarbons
COP	Coefficient of performance
DHW	Domestic hot water
GWP	Global warming potential
HCFC	Hydrochlorofluorocarbons
IWEC	International weather for energy calculation
LMTD	Logarithmic mean temperature difference
ODP	Ozone depletion potential
SH	Space heating
SLHX	Suction line heat exchanger
SPF	Seasonal performance factor
VRC	Volumetric refrigeration capacity



# 1 Introduction

## 1.1 Background

In the last couple of decades there has been an increased focus on the environmental impact of synthetic refrigerants. As a consequence, ozone-depleting CFCs and HCFCs<sup>1</sup> have been phased out with the exception of a few highly specialized ranges of use. HFCs<sup>2</sup> have been introduced as a successor, but due to their high GWP<sup>3</sup> they have a negative impact on climate change when released in the atmosphere. This has led to an increased interest in natural alternatives. CO<sub>2</sub>, also known as R-744 when referred to as a refrigerant, was "rediscovered" as a refrigerant in the 1990s and proposed as an alternative to the synthetic refrigerant by Lorentzen (1994). Being classified as non-flammable, non-toxic and with an GWP and ODP<sup>4</sup> of zero, CO<sub>2</sub> is considered a harmless refrigerant suitable for use in domestic heat pump applications.

## 1.2 Low energy buildings

When evaluating the energy performance of a building, it is important to distinguish between the different forms of energy illustrated in Figure 1.1. Primary energy is the energy extracted directly from nature, and is usually in a form which the end-user cannot directly utilize (Novakovic et al., 2008). Examples of primary energy sources are crude oil, water, wind and solar. This energy must be transformed, transported and distributed before it can be made use of. Secondary energy, or building site energy, is the energy supplied to the building site in a useful form, e.g. refined petroleum products or electricity. The final useful energy, or end-use energy, is the actual energy needed in the building. This would include things like heat, light and mechanical power needed to meet the demands of the building.

---

<sup>1</sup>Chlorofluorocarbons and Hydrochlorofluorocarbons

<sup>2</sup>Hydrofluorocarbons

<sup>3</sup>Global Warming Potential

<sup>4</sup>Ozone Depletion Potential

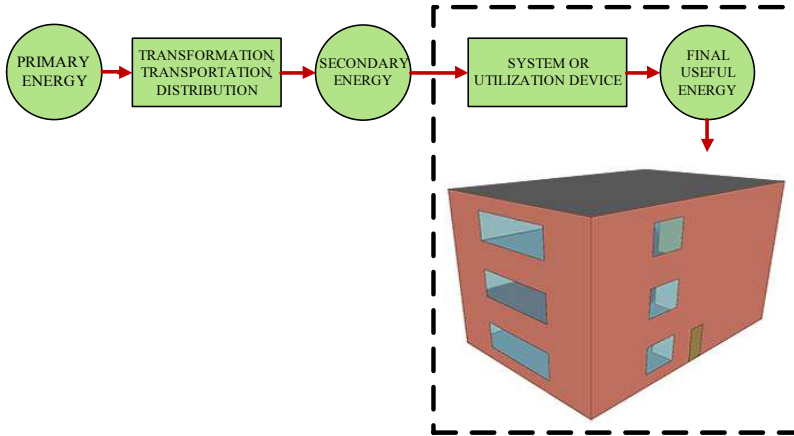


Figure 1.1: *Energy transformation*

In a Norwegian context, a low energy building has to fulfil certain requirements regarding the heat loss from the building and the energy demand and supply of the building. An approach called *passive energy design* has been proposed to fulfil these requirements (Dokka and Hermstad, 2006). In this approach, five steps are to be followed in consecutive order. The steps are summarized in Figure 1.2. The principles are:

1. To reduce the heat loss from the building. This would include choosing low U-value<sup>5</sup> building elements and heat recovery of the ventilation air.
2. To reduce the electric energy consumption by choosing energy efficient appliances and lighting.
3. To locate, orientate and design the building and its facades in such a way as to utilize as much as possible of the free solar energy. Further measures could also include solar collectors or photovoltaic panels.
4. To choose a system that can provide the user with comprehensive and readily available feedback on the building energy demand and usage patterns.

---

<sup>5</sup>The U-value is the overall heat transfer coefficient, a measure on how well heat is conducted through a material.

5. To select an energy source that fits the building demand after all of the aforementioned measures have been taken.

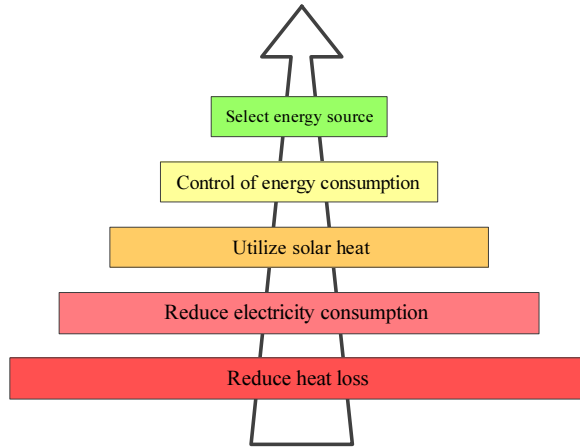


Figure 1.2: *Passive energy design pyramid*

The inclusion of a heat pump in the building energy supply system is a way of reducing the site energy consumption *after* the end-use demands of the building has been reduced. The proposed approach leads to a shift in the energy end-use distribution from being dominated by space heating towards being more evenly distributed between space heating and domestic hot water use. This shift could work in favor of heat pumps using CO<sub>2</sub> as refrigerant as opposed to conventional refrigerants, as the former often achieves better efficiency in domestic hot water applications (Nekså et al., 1998). There is therefore a need for knowledge about the expected performance of these heat pumps under varying operating conditions over the course of a year. Models are however not available in commonly used building energy simulation software.

### 1.3 Objectives

The objectives of this thesis is:

- To do a literature review of CO<sub>2</sub> heat pump technology for use in residential buildings and the integration of CO<sub>2</sub> heat pumps with domestic hot water and space heating systems.
- To develop a CO<sub>2</sub> heat pump model with the aim of integrating it with a whole-building simulation program.
- To determine the optimal parameters for operation in the specific building of interest.
- To analyze the yearly performance of the system under different operating conditions.

The focus of the project is the development of a CO<sub>2</sub> heat pump model that can be used in whole-building energy simulations. Thermal storage is in this study limited to storage of hot water although various other types of thermal storage exist. The economical aspects of installing a heat pump are not treated in this study.



## 2 CO<sub>2</sub> heat pump technology

### 2.1 CO<sub>2</sub> as a refrigerant

#### 2.1.1 Properties of CO<sub>2</sub>

Some of the fundamental physical properties of CO<sub>2</sub> have very different characteristics from those of conventional refrigerants. This has consequences for the design of the heat pump, the choice of components and the heat pump control strategy. As can be read from Table 2.1 CO<sub>2</sub> has a relatively low critical temperature and a high critical pressure compared to synthetic refrigerants often found in domestic heat pumps. Also, due to its high vapour pressure the vapour density of CO<sub>2</sub> is considerably higher than for the conventional refrigerants as shown Figure 2.1.

	R744 (CO <sub>2</sub> )	R134a	R410a
Critical temperature [°C]	31.0	101.1	71.4
Critical pressure [bar]	73.8	40.6	49.0
Vapour density at 0°C [kg/m <sup>3</sup> ]	98	14	31
Heat of vaporization at 0°C [kJ/kg]	231	199	221

Table 2.1: *Refrigerant properties (ASHRAE, 2005)*

The heat of vaporization is comparable in size to that of the other refrigerants. This, in combination with the high vapour density, is beneficial because it gives a high VRC. The VRC can be expressed in terms of the vapour density and the specific heat of evaporation as shown in Equation 2.1 (Arora, 2010). With the VRC being inversely proportional to the suction gas volume, a high VRC reduces the necessary compressor displacement volume for any given rate of heat transfer allowing for smaller compressor sizes.

$$VRC = \rho_v \Delta h_{evap} \quad (2.1)$$

Figure 2.2 reveals that the temperature loss with pressure drop for CO<sub>2</sub> is about six to ten times lower than that of the HFCs. This could allow for a higher pressure drop in pipes and heat exchangers while keeping the temperature loss equal to that of synthetic refrigerants. Alternatively, by

using equal pipe dimensions and heat exchanger designs the temperature loss could be significantly reduced. For a CO<sub>2</sub> heat pump and a HFC heat pump of equal capacity Kim et al. (2004) estimate up to 60-70% reduction in pipe inner diameter and a 80-85% smaller compressor displacement volume for the CO<sub>2</sub> heat pump. A reduction in component size and consequently a more compact heat pump unit could be advantageous in residential buildings if the available space is limited.

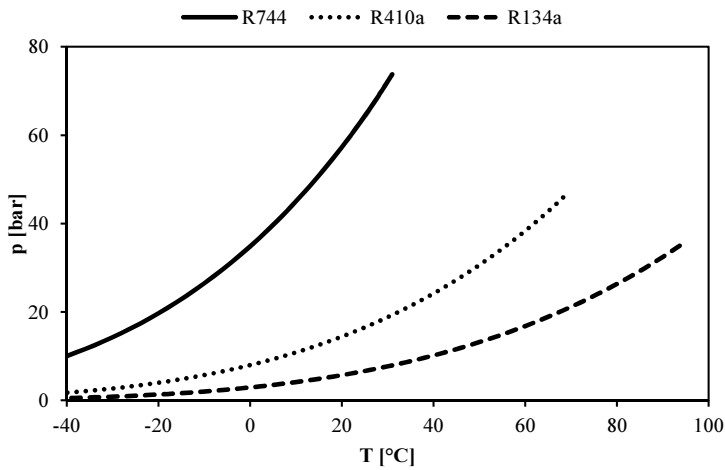


Figure 2.1: *Vapour pressure vs. temperature for selected refrigerants*

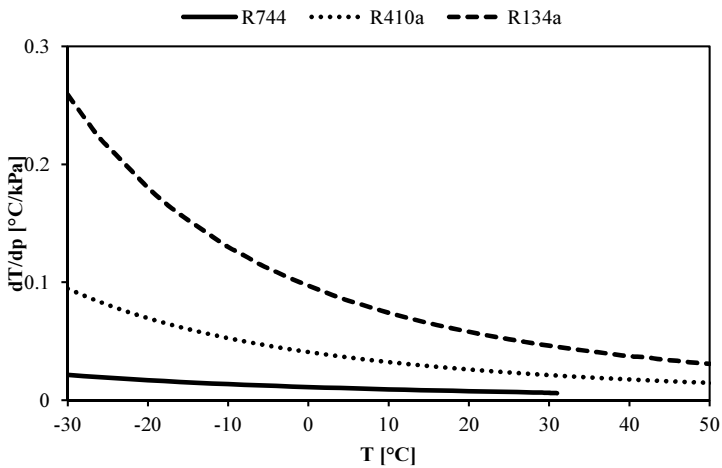


Figure 2.2:  *$\Delta T/\Delta p$  vs. temperature for selected refrigerants*

### 2.1.2 The transcritical CO<sub>2</sub> heat pump cycle

In a conventional heat pump cycle heat is rejected in a subcritical condensation process at a practically constant temperature and pressure. Because of the low critical temperature of CO<sub>2</sub> the practical upper limit of the condensation temperature in a subcritical CO<sub>2</sub> cycle is about 28°C (Stene, 2012a). For residential heating applications like space heating and domestic hot water, where the required temperature level is usually above this limit, the heat pump operates in a transcritical cycle. This cycle differs from the subcritical cycle in that heat rejection occurs at a practically constant pressure, but with varying temperature. In a transcritical CO<sub>2</sub> heat pump system this heat rejection takes place in a *gas cooler*. The ideal Lorentzen cycle was proposed by Halozan and Ritter (as cited by Stene (2004)) as an ideal transcritical CO<sub>2</sub> reference cycle. This cycle consists of the following four processes with numbers referring to Figure 2.3:

- 
- 4-1. Heat absorption at a constant temperature in the evaporator
  - 1-2s. Isentropic compression
  - 2s-3. Heat rejection at a constant pressure in the gas cooler
  - 3-4. Isenthalpic expansion
- 

However, in reality the processes will deviate from those of the ideal reference cycle. Maybe most importantly, a real compressor will have inefficiencies leading to mechanical and thermodynamic losses. Exergy analyses of transcritical heat pumps (Stene (2004), Sarkar et al. (2005)) suggest that compression losses constitute the largest part of the cycle losses. A better representation would therefore take these losses into account. This process is shown as 1-2 in Figure 2.3. However, other studies (Robinson and Groll (1998), Yang et al. (2005)) indicate that the expansion valve is the largest contributor to cycle losses.

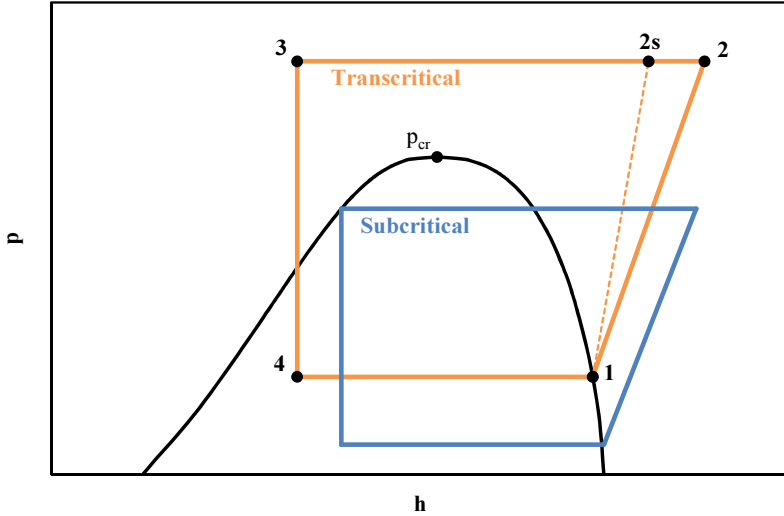


Figure 2.3: *The difference between a transcritical and subcritical cycle illustrated in a pressure-enthalpy diagram*

The COP is a measure of the efficiency with which the heat pump transfers heat to the "hot side" of the system. It is an instantaneous value and is defined as the ratio of the desired heat transfer effect, i.e. the heat rejected in the gas cooler, to the cost in terms of work to accomplish that effect, i.e. the electric input to the compressor (Moran and Shapiro, 2006):

$$COP = \frac{Q_{GC}}{P_C} \quad (2.2)$$

Analogous to the Carnot efficiency, which puts a fundamental limit on the conventional heat pump cycle efficiency, the Lorentz efficiency puts a limit on the efficiency of the transcritical cycle (Stene, 2009):

$$\eta_{LZ} = \frac{COP}{COP_{LZ}} \quad (2.3)$$

Here  $COP_{LZ}$  is the maximum achievable COP for the transcritical process. It is achieved in the case of a reversible process and can be written in terms of the average temperature at which heat rejection occurs in the gas cooler,  $T_m$ , and the temperature of the heat source,  $T_0$ , in [K]:

$$COP_{LZ} = \frac{T_m}{T_m - T_0} \quad (2.4)$$

It is clear that the efficiency is heavily influenced by the temperature at which heat rejection occurs. In the conventional heat pump cycle this temperature equals the constant temperature in the condenser. For the transcritical cycle, where the heat rejection occurs at varying temperatures, the average temperature  $T_m$  will be somewhere in between the  $\text{CO}_2$  temperature at the inlet of the gas cooler and the temperature at the outlet of the gas cooler. In order to achieve a high COP it is desirable to keep the average temperature as low as possible. The *outlet* temperature of the secondary fluid from the gas cooler is generally set to a desired value. Therefore, the *inlet* temperature of the secondary fluid to the gas cooler will to a large extent determine the average  $\text{CO}_2$  temperature and thus the COP of the transcritical cycle. The influence of the average heat rejection temperature is illustrated in Figures 2.4 and 2.5. When the temperature glide of the secondary fluid is small, the conventional heat pump achieves a higher COP than the  $\text{CO}_2$  heat pump. This is because the temperature in the condenser can be kept lower than the average temperature in the gas cooler for the same amount of heat transfer as illustrated in Figure 2.4.

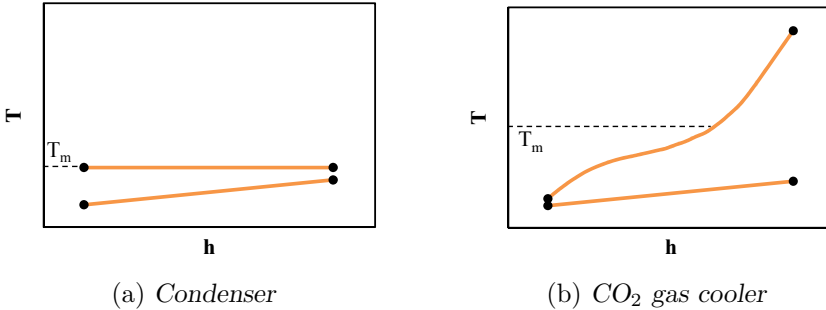


Figure 2.4: Illustration of the average heat rejection temperature at small temperature glide in a temperature-enthalpy diagram

The opposite is the case when the temperature glide of the secondary fluid is large. Then the good temperature glide fit of  $\text{CO}_2$  and the secondary fluid in the gas cooler means that the  $\text{CO}_2$  heat pump can achieve a lower

average temperature and thus a higher COP than that of the conventional heat pump as illustrated in Figure 2.5.

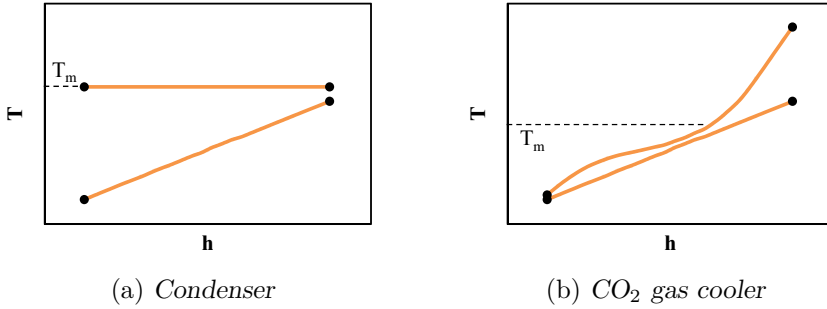


Figure 2.5: Illustration of the average heat rejection temperature at large temperature glide in a temperature-enthalpy diagram

The non-linearity of the  $CO_2$  temperature glide is due to the strongly varying specific heat near the critical point. Figure 2.6 shows how the specific heat varies with temperature at different supercritical pressures. The variation gets smaller with increasing pressure and the specific heat is nearly constant at very high pressures. The strongly varying properties of  $CO_2$  make the gas cooling process distinguishably different from the conventional condensation process and would be of importance in gas cooler modeling.

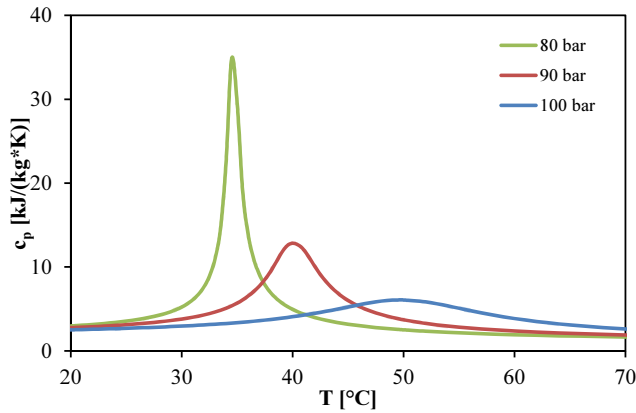


Figure 2.6: Specific heat of  $CO_2$  as a function of temperature at supercritical pressures

## 2.2 Heat pump design

The most basic transcritical heat pump consists of four main components; An evaporator, a compressor, a gas cooler and an expansion valve. The refrigerant, in this case CO<sub>2</sub>, is circulated in a closed circuit made up by these components and the pipes connecting them. Figure 2.7 shows an illustration of a heat pump with the points 1 to 4 referring to Figure 2.3. The gas cooler in an air-to-water heat pump is typically a concentric tube-in-tube heat exchanger with a counter flow arrangement (Austin and Sumathy (2011), Goodman et al. (2011)).

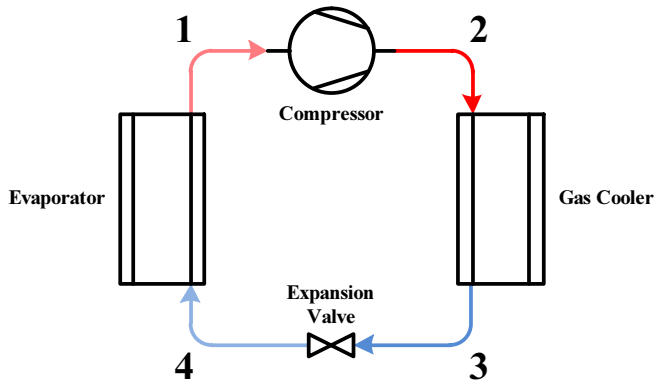


Figure 2.7: *Principle of a transcritical heat pump*

The compressor performance is often described by volumetric and isentropic efficiencies which are mainly influenced by the pressure ratio  $p_2/p_1$  in Figure 2.3 (Cecchinato et al., 2011). Different types of compressors exist which are able to operate either at a single speed, at one or more fixed-step speeds or at a continuously variable speed. The latter two types are generally preferred because they make it possible to match the heat pump heat capacity to the building demand resulting in better part-load performance. However, these compressor are often more expensive and require more complex system controls in order to take advantage of the variable speed. Karlsson (2007) compares the performance of a conventional heat pump with a single-speed compressor to that of one with a variable-speed compressor. A significant performance increase is estimated in the case of the variable-speed system provided optimized

controls of the compressor and circulation pumps. Because the same principle of matching the load and capacity applies, there is reason to believe that significant energy savings could be made by utilizing variable speed control also for a transcritical heat pump.

Various modifications can be made to the basic system in order to improve the heat pump performance. A liquid receiver and a suction line heat exchanger are the most common modifications (Austin and Sumathy, 2011), and can be incorporated as shown in Figure 2.8. The receiver is placed on the suction line before the compressor inlet and ensures that no liquid enters the compressor. It also acts as a buffer, enabling control of the gas cooler pressure. The refrigerant mass flow rate through the valve can be momentarily increased or decreased by adjusting the expansion valve opening. This leads to a new balance between valve flow rate and compressor flow rate and consequently a pressure change in the gas cooler (Kim et al., 2004), and opens for the opportunity to regulate the gas cooler pressure in order to achieve optimal conditions for heat transfer. The suction line heat exchanger improves the cycle efficiency by enabling heat transfer between the gas exiting the gas cooler and the gas entering the compressor.

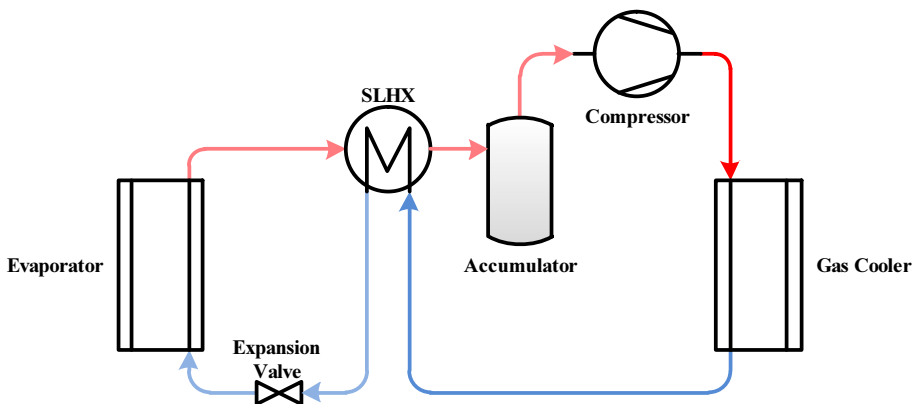


Figure 2.8: *Basic transcritical heat pump modified with a liquid receiver and a suction line heat exchanger (SLHX)*

Modifications can also be made in order to improve cycle performance by the use of various types of expander devices for the expansion process. In this way some of the expansion work can be recovered. The effect



of this is thought to be greater for transcritical heat pumps than for conventional heat pumps because of the large pressure difference between the low pressure side and the high pressure side in the transcritical cycle (Austin and Sumathy, 2011). Experiments have however indicated that such expander devices could be less effective when used in combination with a SLHX (Xu et al., 2011).

### 2.3 Integration with thermal storage and space heating systems

In a CO<sub>2</sub> heat pump system for use in residential buildings, the gas cooler(s) can be either placed externally or integrated into a hot water tank. Different configurations incorporating either a single or multiple gas coolers are possible in order to take full advantage of the temperature glide. The most basic configuration is that the heat rejection takes place through a single gas cooler as in Figure 2.9. It is cheaper and less technically complex than a system with multiple gas coolers and would be best suited in the case of a demand for a single temperature level, e.g. in the case of a heat pump water heater for heating of domestic hot water (DHW) only.

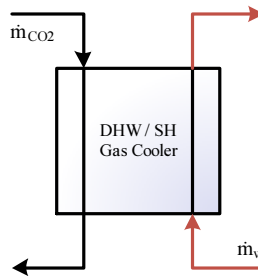


Figure 2.9: *Single gas cooler configuration*

A single external gas cooler can also be utilized when there is a demand for both space heating (SH) and DHW. Figure 2.10 shows possible system solutions incorporating a storage tank for DHW and heat exchanger(s) for SH. The heat exchanger can be either outside the storage tank as in Figure 2.10a or integrated in the storage tank. If water at different

temperature levels is required, either for SH or for other purposes, a combination of both as shown in Figure 2.10b could also be used.

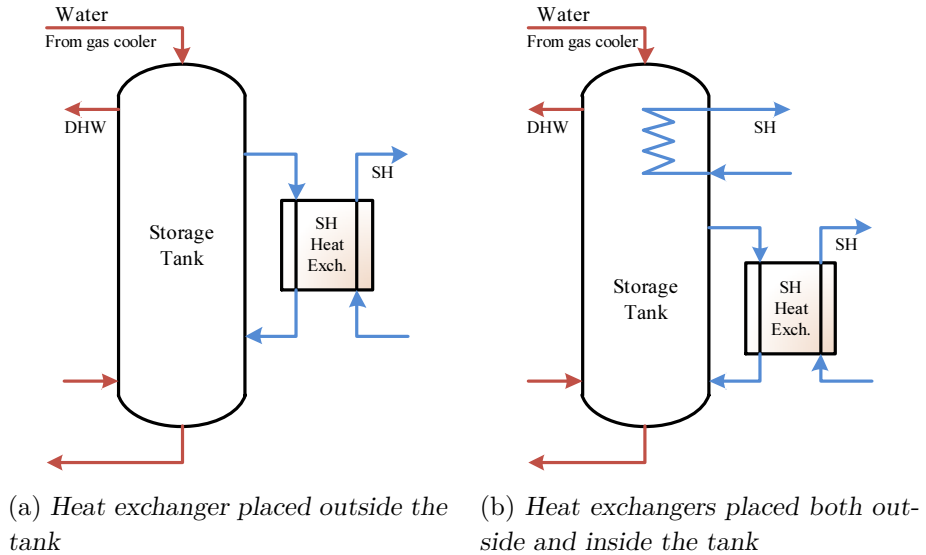


Figure 2.10: Single gas cooler connected to a storage tank

A bipartite gas cooler consisting of two separate units can be beneficial when there is a demand for heat at different temperature levels, which is often the case for DHW and SH. Figures 2.11 and 2.12 illustrate different ways of incorporating two gas cooler units, one for DHW and one for SH. In Figure 2.11a the gas cooler units are connected in series with the DHW gas cooler located before the SH gas cooler. High temperature SH is not possible with this configuration because of the location of the SH gas cooler, and the minimum  $\text{CO}_2$  outlet temperature is limited by the return temperature from the SH distribution system. Placing the DHW gas cooler after the SH gas cooler, as in Figure 2.11b, allows for high temperature SH. This configuration excludes the possibility of high temperature DHW so there would be a need for reheating of the DHW by other means, but the minimum  $\text{CO}_2$  outlet temperature is equal to the water mains temperature and thus lower than that of configuration 2.11a. Figure 2.12 shows the gas coolers connected in parallel. This configuration allows for simultaneous high temperature SH and DHW heating. The  $\text{CO}_2$  outlet temperature is determined by the water mass

flow through each of the gas coolers and will be somewhere between the water mains temperature and the return temperature from the SH distribution system (Stene, 2009).

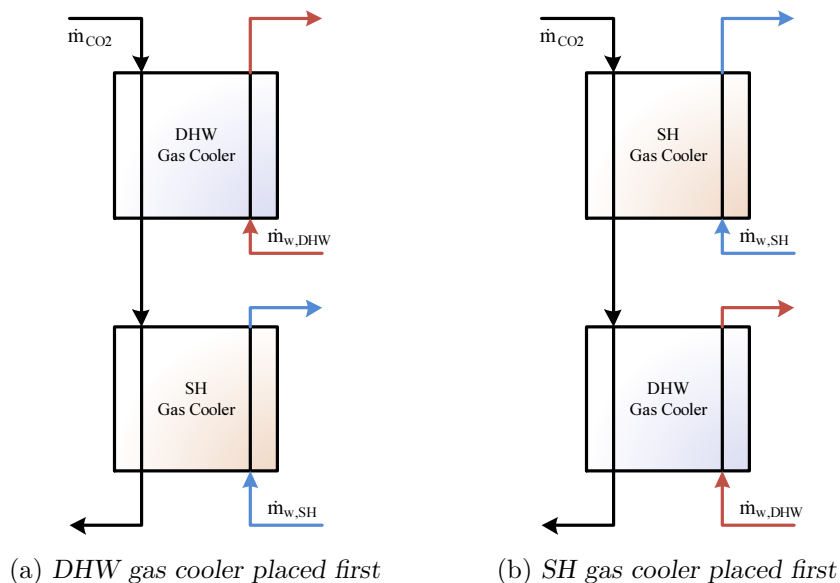


Figure 2.11: Bipartite gas cooler in series configuration

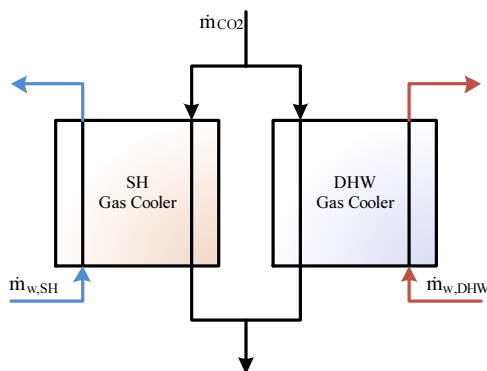


Figure 2.12: Bipartite gas cooler in parallel configuration

While being a more complex configuration, a tripartite gas cooler consisting of three units as shown Figure 2.13 allows preheating of DHW, low temperature SH and reheating of DHW. The minimum CO<sub>2</sub> outlet

temperature equals the water mains temperature in both DHW mode and combined mode (simultaneous DHW and SH demand), taking full advantage of the the temperature glide when cooling the CO<sub>2</sub>. In SH mode the minimum temperature equals the return temperature of the SH system.

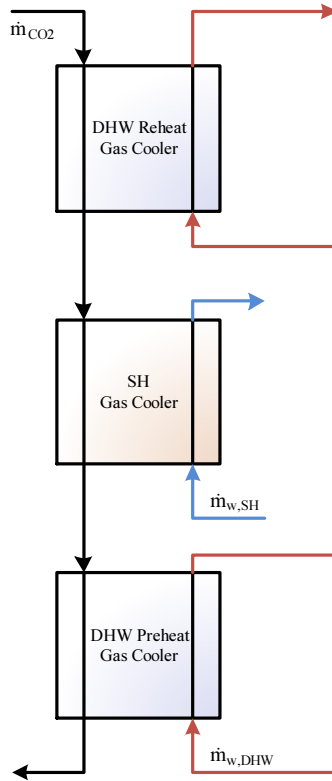


Figure 2.13: *Tripartite gas cooler configuration*

For compactness the gas cooler(s) can be integrated into the storage tank. Figure 2.14 shows a couple of possibilities for placing the gas cooler(s) internally. Figure 2.14a bears a resemblance to Figure 2.10a where the water for SH is also heated through an external heat exchanger, but in Figure 2.14a the gas cooler is placed internally in the DHW tank. In Figure 2.14b the system consists of three gas cooler units similar to that of Figure 2.13, but with the DHW gas cooler units placed internally in the tank. The drawback with these configurations is that the advantage of the external gas cooler counter-flow arrangement is lost. The COP

is therefore generally lower than that of the external gas cooler systems (Stene, 2009).

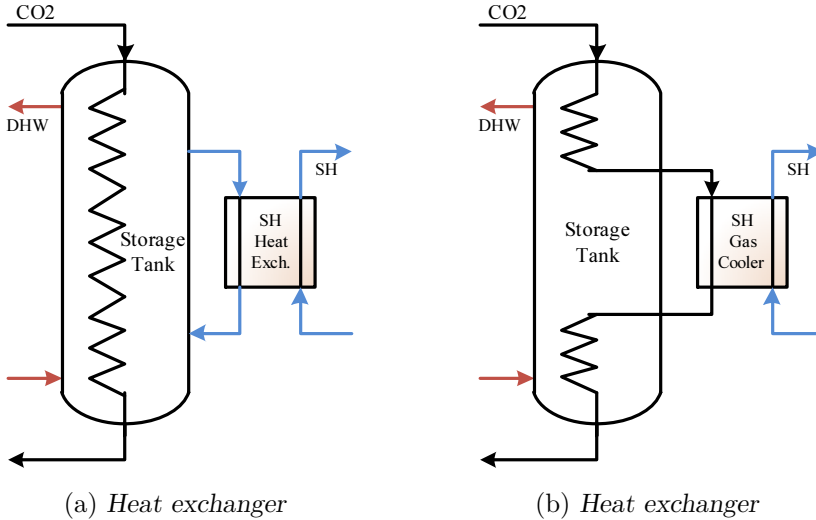


Figure 2.14: Internal gas cooler configurations

### 2.3.1 Domestic hot water

Application of the passive energy design principles of Figure 1.2 leads to a reduction of the transmission and infiltration losses through the building envelope, reducing the annual space heating demand. The DHW demand depends mainly on the building usage pattern and stays relatively constant independent of the building envelope, which means that the *relative* DHW heating demand, the ratio of the annual DHW heating to space heating, increases. As discussed in Chapter 2.1 one of the strong points of the CO<sub>2</sub> heat pump is the high performance when there is a relatively large temperature glide involved, as is the case with DHW. This could make the CO<sub>2</sub> heat pump very well suited for heating of DHW in low energy buildings. In addition, the reduction of component size in CO<sub>2</sub> heat pump systems as compared to conventional heat pump systems can be advantageous in residential applications, especially in urban areas where space could be limited.

The large influence of the CO<sub>2</sub> outlet temperature from the gas cooler on the COP makes a low water inlet temperature to the gas cooler desirable, cooling the CO<sub>2</sub> gas as much as possible. The lowest possible water inlet temperature is determined by the supply water from the DHW storage tank. Heat transfer by mixing and conduction between the hot and cold water in the tank increases the supply temperature, and is therefore undesirable. Stene (2004) investigates the effect of placing a moving insulating plate inside the tank as illustrated in Figure 2.15. It is demonstrated that by separating the water into a hot and a cold part like this the heat transfer between the two parts could be reduced with about 80%. Furthermore it is suggested that the system performance will benefit from having an inlet flow diffuser and a high diameter-to-height ratio in order to minimize mixing and conductive heat transfer inside the tank, as better thermal stratification in the tank will help keeping the gas cooler inlet water temperature low.

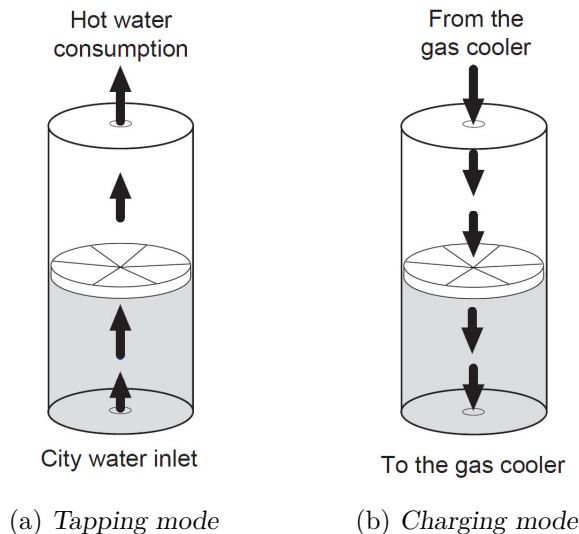


Figure 2.15: DHW tank with a moving insulating plate separating the hot and cold water (Stene, 2004)

Fernandez et al. (2010) evaluate the performance of a CO<sub>2</sub> heat pump water heater over the course of heating a full hot water tank. No performance enhancing modifications are incorporated and the heat pump therefore has a basic configuration resembling that of Figure 2.7. Three

different cases are tested:

- 
1. Heating a tank initially filled with cold water at 15°C
  2. Reheating a tank after tap water has been drawn
  3. Reheating a tank after standby losses
- 

In cases (2) and (3) the cut-in temperature at which heating of the tank starts is 42.2°C, and the water is then heated to 57.2°C. The thermal stratification in the tank is found to be greater in case (2) than in case (3) because hot water is drawn from the top of the tank and then cold water is refilled at the bottom of the tank. Case (2) provides a lower gas cooler water inlet temperature than in case (3) and thus more favorable conditions for the heat pump. In case (2) the COP ranges from about 2.5 to 3.3 at outdoor air temperatures of 10 to 30°C. This is somewhat lower than in case (1) where the COP ranges from about 2.8 to 3.8, but significantly higher than in case (3) where the COP ranges from about 2.0 to 2.6. This indicates that performance degradation could be reduced by minimizing the standby losses and taking the necessary measures to ensure good thermal stratification in the tank.

### **2.3.2 Hydronic space heating**

Efficient operation of a transcritical heat pump in the building energy supply system sets requirements to the heat distribution system. For space heating the minimum achievable gas cooler CO<sub>2</sub> outlet temperature equals the return temperature of the heat distribution system. It is therefore generally desirable with a low supply and return temperature for the space heating system for the reasons discussed in Chapter 2.1.2. For the space heating system a number of solutions exists with underfloor heating commonly being utilized, but other options like fan coils and convectors also exist. According to Halozan (1997) the supply temperature in a building with reduced heating demand could typically be in the range of 30-35°C. It is further suggested that a more efficient design of the underfloor system could make supply temperatures as low as 27-32°C possible. Based on measurements from a prototype CO<sub>2</sub> heat pump Stene (2004) reports an 8% increase in COP when decreasing the supply/return temperatures from 40/35°C to 35/30°C. A further

5% increase in COP is achieved when decreasing the temperatures from 35/30°C to 33/28°C.

An accumulator tank can be utilized to act as a thermal storage for the space heating system, providing a more stable supply temperature. The heat pump may also benefit from this by decoupling the water flow in the heating system from the water flow in the gas cooler eliminating the need for starting and stopping the compressor at low loads. However it has been suggested that by taking some preemptive measures this benefit would be rather small (Uhlmann and Bertsch, 2012). It also introduces increased system and controls complexity and increased investment costs due to additional components.

## 2.4 System performance

The COP is only a measure of the heat pump performance at any given operating condition, so when evaluating the performance of the heat pump there is a need for a measure of performance over a period of time. The *seasonal performance factor* provides a measure of the performance over a period of time, e.g. over a full year. It is defined as:

$$SPF = \frac{\text{Heat delivered from heat pump}}{\text{Electrical energy supplied to heat pump}} \quad (2.5)$$

An important thing to take note of is that energy savings are not proportional to the SPF. Increasing the performance of a low-SPF heat pump system will give a larger relative energy saving than increasing the performance of a high-SPF system. Equation 2.6 gives the relative energy savings for a heat pump system where  $\lambda$  is the fraction of annual demand covered by the heat pump. The energy savings are in comparison to an alternative heating system/peak load system with an efficiency of  $\eta$ . In further comparisons the alternative system is assumed to be an electrical heating system with 100% efficiency. Figure 2.16 shows the relative energy savings as a function of heat pump SPF when the heat pump covers 70%, 90% and 100% of the annual demand.

$$\Delta E = \left(\frac{1}{\eta}\right) - \left(\frac{\lambda}{SPF}\right) - \left(\frac{1-\lambda}{\eta}\right) \quad (2.6)$$



The optimum heating load coverage for the heat pump is determined by a number of factors including the climate at the building site, the building usage pattern, the heat pump performance at different operating conditions and investment and operating costs. A coverage of 40-70% of the peak heating load is typical for the dimensioning of the heat pump, resulting in about 90% coverage of the annual heating demand (Novakovic et al., 2008).

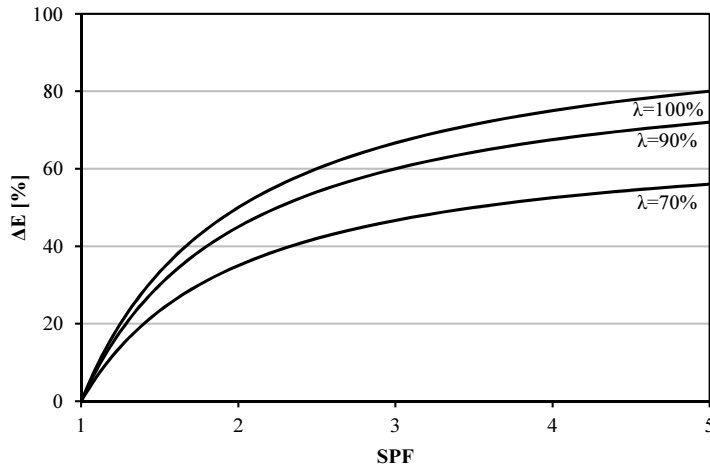


Figure 2.16: *Relative energy savings as a function of SPF for a heat pump system covering 100%, 90% and 70% of annual demand,  $\eta = 1$ .*

The equivalent operating time of the heat pump says something about how well the capacity of the heat pump is being utilized. A low equivalent operating time could indicate that the heat pump is operating at part load, or not at all, during significant time periods of the year. It is defined as:

$$\tau = \frac{E_{HP}}{Q_{HP}} \quad (2.7)$$

Where  $E_{HP}$  is the total heat delivered from the heat pump and  $Q_{HP}$  is the rated heating capacity of the heat pump at design conditions. The equivalent operating time for residential heat pumps are often in the range of 2000 to 4000 hours (Stene, 2012b).



### 3 Transcritical heat pump models in literature

Heat pump models generally fall into one of two categories; equation-fit or deterministic (Hamilton and Miller, 1990). The former requires heat pump performance data for a large number of operating points, and often perform poorly when extrapolating beyond the range of the performance data. However the required data are often readily available (e.g. heating capacity or compressor performance curves) and they could be very well suited when operating conditions are well known and the inner workings of the heat pump are not of interest. Because they have the tendency to fall short when operating over a large range of conditions and provide relatively little insight into factors of interest during operation, it was decided to focus on the latter of the two categories in this study.

Deterministic models are based on fundamental thermodynamic equations and can model each heat pump component with a varying degree of complexity. Numerous transcritical heat pump models have been proposed, and the purpose of these models is often to assess the operating characteristics of a specific heat pump. They therefore often require detailed knowledge of heat pump component specifications. For whole-building simulations many variables are involved in modeling the interactions between the building, the energy supply system and the environment. The more complex models could here provide more accuracy than actually needed, and they are also generally more computationally expensive. The following is a review of a selection of models that were considered suitable for inclusion in a building simulation environment. They have many similarities, e.g. they are all based on fundamental thermodynamic equations for each heat pump component, but they have a varying degree of complexity and require different input parameters.

#### 3.1 Brown and Domanski (2000)

Brown and Domanski (2000) present a simulation model for a transcritical mobile airconditioning system. Although it is designed for automotive cooling purposes it operates under very similar conditions as a heat pump for residential heating would, and could therefore be of interest in this study. An internal suction gas heat exchanger is incorporated

in the system making it similar to that of Figure 2.8. The evaporator and gas cooler are both assumed to have a constant overall heat transfer coefficient. In the case of the gas cooler this is a very rough approximation because of the strongly varying properties of CO<sub>2</sub> during the cooling process as discussed in Chapter 2. The compressor performance is determined from the electric efficiency, speed and displacement volume. The model takes the pressure drop through the evaporator and gas cooler into account, either by imposed user input values or by simulated values. In the latter case the transport properties of CO<sub>2</sub> are used for calculating the pressure drops. Simulation results show that the COP deviates with up to 13.4% and the heating capacity with up to 21.4% from experimental data.

### 3.2 Stene (2004)

Stene (2004) investigates the performance of a 6.5 kW transcritical heat pump test rig incorporating a tripartite gas cooler like that of Figure 2.13 for space heating and DHW preheating/reheating, in addition to a suction gas heat exchanger. A computer model of the test rig is developed. This is a more detailed model than that of Brown and Domanski (2000) taking into account the geometry of the heat exchangers and the transport properties of CO<sub>2</sub>. It also divides the gas cooler into multiple subsections in order to take into account the varying properties of CO<sub>2</sub> during cooling. The properties are kept constant within each subsection so that the temperature profile of CO<sub>2</sub> through the gas cooler are approximated in discrete steps. A number of 20 subsections is suggested as adequate in order to achieve a good representation of the CO<sub>2</sub> temperature profile in the gas cooler. The compressor is modeled from Equation 3.1 with the discharge state being determined from the compressor suction state, isentropic efficiency  $\eta_{is}$  and a heat loss factor  $\beta$  with states 1, 2 and 2s referring to Figure 2.3.

$$h_2 = h_1 + \frac{h_{2s} - h_1}{\eta_{is}}(1 - \beta) \quad (3.1)$$

Simulations show very small deviations from experimental results over the tested range, with a maximum of 1% deviation from experimental

data in the case of both COP and heating capacity. However taking into account the heat exchanger geometry requires detailed knowledge about the specific component used, and might be "overkill" for the purpose of building simulations where there is a lot of other factors influencing the final simulation results.

### 3.3 Sarkar et al. (2006)

Sarkar et al. (2006) develop a transcritical heat pump model for simultaneous heating and cooling. The gas cooler is divided into subsections and the LMTD method (Rohsenow et al., 1998) is then employed in each subsection similar to the approach of Stene (2004). In this model the evaporator is treated in the same manner. The compression process is assumed to be adiabatic with the volumetric and isentropic efficiencies expressed as functions of the compression ratio. The method of expressing the volumetric and isentropic efficiencies as functions of the pressure ratio would expectedly give a more realistic representation of the compressor performance than an assumption of constant values, especially if there is a large variation in pressure ratio in the range of operation.

### 3.4 Yokoyama et al. (2007)

Yokoyama et al. (2007) simulate a heat pump water heating system including a hot water storage tank. The system is modeled on a component level. Pressure drop throughout the gas cooler is neglected and the overall heat transfer coefficient is assumed to be constant. Neglecting the gas cooler pressure drop could be justified by the generally low relative pressure drop and accompanying temperature drop under transcritical conditions, and together with the assumption of constant overall heat transfer coefficient it would eliminate the need for knowledge about heat exchanger geometry. The gas cooler is divided into  $N$  subsections of equal heat exchanger area so that the overall heat transfer coefficient in subsection  $j$  is:

$$UA_j = \frac{UA_D}{N} \quad (3.2)$$

Within each subsection the thermodynamic properties of water and CO<sub>2</sub> are assumed constant, and the LMTD method is applied in order to determine the heat transfer between the CO<sub>2</sub> gas and the water. The compressor model is similar to that of Stene (2004) and takes into account the volumetric isentropic efficiencies and the heat loss from the compressor. However, the mass flow rate through the compressor is described by a quadratic relation derived from experimental data from a specific heat pump. Simulation results from this model show a good agreement with experimental results over a large range of operating conditions.

### 3.5 Cecchinato et al. (2011)

Cecchinato et al. (2011) propose a mathematical model of a heat pump water heater with an internal suction gas heat exchanger. The model requires various performance data, including secondary fluid data, at design conditions. It also requires the heat exchanger design ratios of refrigerant surface area to secondary fluid area ( $A_r/A_{sf}$ ) and refrigerant heat transfer coefficient to secondary fluid heat transfer coefficient ( $U_r/U_{sf}$ ) to be known. Other parameters at design conditions are then calculated from these data. The gas cooler is divided into  $N$  subsections and the P-NTU method (Rohsenow et al., 1998) is used along with a correction factor to calculate the heat transfer in subsection  $j$ :

$$NTU_j = \left( \frac{UA_D k}{C} \right)_j \quad (3.3)$$

Where the correction factor  $k$  is a function of the mass flows, heat transfer coefficients and heat exchanger areas of the refrigerant and secondary fluid. The evaporator is treated in a similar manner. The compressor discharge state is determined from the compressor suction state, isentropic efficiency and heat loss factor similar to that of Stene (2004). A partialisation factor is introduced in the case of a variable speed compressor. For part load operation the volumetric and isentropic efficiencies are then treated as functions of the compressor pressure ratio and a partialisation factor. The calculated COP and heating capacity of an air-to-water heat pump deviate from experimental results with -6.8% to 1.7% and -5.5% to 1.7% respectively. The need for detailed knowledge of component

specifications, geometry etc. could limit the use of this model in building energy simulations where often relatively limited catalog data are available.

### **3.6 Yamaguchi et al. (2011)**

Yamaguchi et al. (2011) present a very detailed transcritical heat pump model incorporating an internal heat exchanger. The gas cooler refrigerant-side heat transfer coefficient calculations are based on correlations proposed by Dang et al. (2007) which takes into account detailed heat exchanger geometry and the effects of lubricating oil requiring detailed input data, and the pressure drop due to friction loss and fluid density change are also taken into account. The evaporator is divided into multiple zones of different flow patterns on the refrigerant side, with appropriate correlations for the heat transfer coefficient and pressure drop applied to each zone.

The compressor is modeled similar to that of Sarkar et al. (2006) with volumetric, isentropic and adiabatic efficiencies as functions of the compressor pressure ratio determined from experimental data. The iteration process in this model differs somewhat from that of the other models described. Here, instead of a successive calculation of inlet and outlet states, the inlet states of each component are guessed and the outlet states are calculated. This is repeated in an iterative process until reaching a satisfying conformity between the outlet state of one component and the inlet state of the next. Simulation results are shown to be accurate over a range of operating conditions, with the maximum difference in the COP between simulation and experimental results being 5.4% and the average difference being 0.9%.

### **3.7 Control of gas cooler pressure**

Lorentzen (1994) suggests that for any operating condition there exists an optimal gas cooler pressure which gives the highest COP. Several papers (Liao et al. (2000), Chen and Gu (2005), Sarkar et al. (2004)) deal with determining the optimal gas cooler pressure as a empirical correlations obtained from experimental data. As discussed in Chapter 2 the

gas cooler CO<sub>2</sub> outlet temperature is a major factor influencing the heat pump performance. Liao et al. (2000) find that the optimal gas cooler pressure depends mainly on the gas cooler CO<sub>2</sub> outlet temperature, the evaporation temperature and the compressor characteristics. The problem is then further reduced with the assumption of constant compressor efficiency so that:

$$p_{GC,opt} = f(T_{GC,CO_2,o}, T_{E,CO_2}) \quad (3.4)$$

It is further shown that the dependence of the optimal pressure on the gas cooler CO<sub>2</sub> outlet temperature is much greater than that on the evaporation temperature. This is supported by Sarkar et al. (2004) who present the optimum gas cooler pressure for evaporator temperatures ranging from -10°C to 10°C and CO<sub>2</sub> outlet temperatures from 30°C to 50°C. It is also shown that the dependence on the evaporator temperature decreases at lower evaporator temperatures. A reasonable strategy could therefore be to control the gas cooler pressure based on the CO<sub>2</sub> outlet temperature or the secondary fluid inlet temperature with which the CO<sub>2</sub> outlet temperature is closely related. This is the approach taken by Chen and Gu (2005) who investigate the optimum pressure for a transcritical refrigeration system. They propose a linear correlation between the gas cooler CO<sub>2</sub> outlet temperature and the optimal pressure, and it is demonstrated that this correlation predicts the optimal gas cooler pressure with a maximum deviation of 3.6% from the actual optimum with evaporator temperatures varying from -10°C to 10°C and CO<sub>2</sub> outlet temperatures varying from 30°C to 50°C. Qi et al. (2013) investigate the optimal pressure of a transcritical heat pump water heater. The proposed cubic correlation between the CO<sub>2</sub> outlet temperature and the optimal pressure is shown to predict the pressure within ±5% of the actual optimum with ambient temperatures ranging from -15°C to 30°C and CO<sub>2</sub> outlet temperatures from 25°C to 45°C. The forementioned studies all cover a narrower range of gas cooler CO<sub>2</sub> outlet temperatures than is of interest in this current study, and they only investigate the optimal pressure for water demand at a single temperature level. It is therefore uncertain with which accuracy similar correlations are able to predict the optimal gas cooler pressure in the case of a full year building simulation with varying temperature demands for DHW and space heating.



## 4 Development of a transcritical heat pump model

### 4.1 Heat pump model

A heat pump model was developed taking basis in Figure 2.7 and the models outlined in Chapter 3. The pressure drop through the expansion valve was considered isenthalpic so that the evaporator inlet enthalpy equaled the gas cooler outlet enthalpy (points 4 and 3 respectively in Figure 4.1). For the evaporator, process 4-5 in Figure 4.1, the heat loss to the surroundings was assumed to be negligible, and the temperature and pressure of CO<sub>2</sub> were assumed to be constant throughout the heat exchanger. The specific heats of both the refrigerant and the secondary fluid were also assumed to be constant. The  $\varepsilon$ -NTU method (Rohsenow et al., 1998) was employed, which for a heat exchanger with phase change occurring on one side takes the form of Equation (4.1). The total heat transfer in the evaporator was then calculated from Equation (4.2).

$$\varepsilon_E = 1 - e^{-NTU_E}, \quad NTU_E = \frac{UA_E}{C_{sf,E}} \quad (4.1)$$

$$Q_E = \varepsilon_E C_{sf,E} (T_{r,E} - T_{sf,E,i}) \quad (4.2)$$

For the compressor model the possibility of specifying a constant superheat temperature value and an isenthalpic suction line pressure drop value before the compressor inlet was included. From this the compressor suction state, point 1' in Figure 4.1, could be established. The superheat and suction line pressure drop are shown in Figure 4.1 as process 5-1 and 1-1' respectively. The mass flow rate of CO<sub>2</sub> was calculated from the volumetric efficiency, the compressor suction state and the displacement rate by Equation 4.3. The compressor was assumed to operate intermittently at a single speed (i.e. at a constant displacement rate).

$$\dot{m}_r = \eta_{vol} \rho_1 \dot{V} \quad (4.3)$$

Analogous to the model by Stene (2004) the compressor discharge state, point 2' in Figure 4.1, was determined using Equation 3.1. The total power input and the compressor work on the gas were then calculated from Equations 4.4 and 4.5. The volumetric and isentropic efficiencies were both assumed to be constant throughout the compressor range of operation.

$$P_C = \dot{m}_r \frac{h_{2s} - h_1}{\eta_{is}} \quad (4.4)$$

$$W_C = P_C - W_{loss} = \dot{m}_r \frac{h_{2s} - h_1}{\eta_{is}} (1 - \beta) \quad (4.5)$$

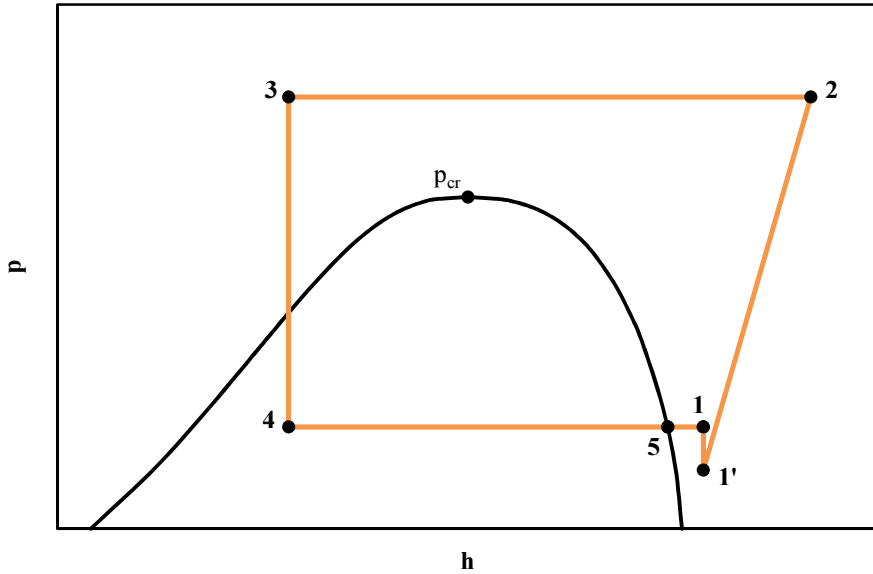


Figure 4.1: *The modeled heat pump process illustrated in a pressure-enthalpy chart*

The gas cooler model was similar to that of Yokoyama et al. (2007). This model demonstrated good agreement with experimental results compared to the simpler model of e.g. Brown and Domanski (2000), while still being simple enough to incorporate relatively pain-free into a whole building simulation environment. Heat loss to the surroundings and pressure drop

through the gas cooler were both assumed to be negligible. A constant overall heat transfer coefficient was assumed, and the gas cooler was then divided into  $N$  subsections so that the overall heat transfer coefficient of each subsection took the form of Equation 3.2. By division of the gas cooler into subsections the strongly varying properties of  $\text{CO}_2$  during cooling as discussed in Chapter 2.1.2 could be accounted for. A model also taking transport properties into account, like the one by Cecchiato et al. (2011), was thought to give a better representation but also to complicate the model by requiring more detailed data and calculations. There was also some uncertainty associated with the possibility of integrating the more complicated model into EnergyPlus. Figure 4.2 illustrates the division of the gas cooler into subsections, while Figure 4.3 shows the control volume of *one* subsection. Here,  $T_{r,N}$  would denote the  $\text{CO}_2$  inlet temperature and  $T_{sf,0}$  the secondary fluid inlet temperature. The thermodynamic properties of the secondary fluid were assumed to be constant throughout the gas cooler, while the properties of  $\text{CO}_2$  were assumed to be constant *within each subsection* and were evaluated at the arithmetic mean temperature:

$$T_{avg,r,j} = T_{r,j-1} + \frac{T_{r,j} - T_{r,j-1}}{2} \quad (4.6)$$

With an assumed counterflow arrangement, the effectiveness of subsection  $j$  took the form of Equations (4.7) – (4.9) (Rohsenow et al., 1998). The heat transfer rates and the secondary fluid outlet temperature were then calculated using the energy Equations (4.10) – (4.12):

$$\varepsilon_j = \frac{1 - e^{-NTU_j(1-C_{r,j})}}{1 - C_{r,j}e^{-NTU_j(1-C_{r,j})}}, \quad C_{r,j} < 1 \quad (4.7)$$

$$\varepsilon_j = \frac{NTU_j}{1 + NTU_j}, \quad C_{r,j} = 1 \quad (4.8)$$

$$NTU_j = \frac{UA_j}{C_{\min,j}} \quad (4.9)$$

$$Q_j = \varepsilon_j C_{\min,j} (T_{r,j} - T_{sf,j-1}) \quad (4.10)$$

$$Q_{r,j} = C_{p,r,j} (T_{r,j} - T_{r,j-1}) \quad (4.11)$$

$$T_{sf,j} = T_{sf,j-1} + \frac{Q_j}{C_{sf}} \quad (4.12)$$

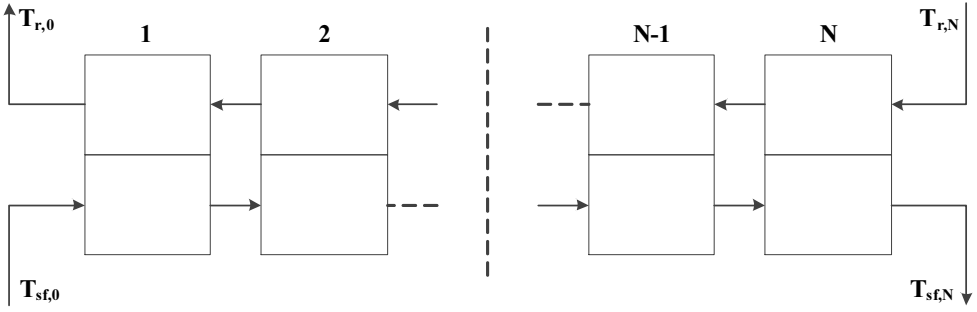


Figure 4.2: *Illustration of the gas cooler subsection division*

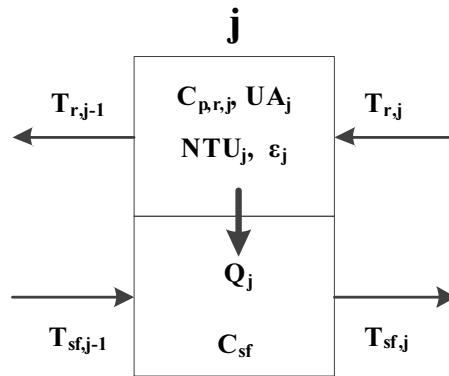


Figure 4.3: *Illustration of one gas cooler subsection*

A linear temperature profile in the gas cooler was used as an initial guess, and the temperature profile was then updated for each consecutive subsection calculation. A convergence criterion was set for the gas cooler model so that iterations would continue until the difference between the heat transfer rate on the CO<sub>2</sub> side and the secondary fluid side was less than 1% in each subsection. A flowchart for the gas cooler calculations are shown in Figure 4.4b. The overall heat pump model started with an initial guess of no heat transfer (i.e.  $Q_{GC}$  and  $Q_E$  equals zero) so that the evaporator temperature equaled the heat source temperature. For the overall heat pump model the iterations continued until the change in heat transfer rates for the gas cooler and evaporator were less than 0.1%. The calculation algorithm for the overall heat pump model, in which the gas cooler calculation step is included, is shown in Figure 4.4a.

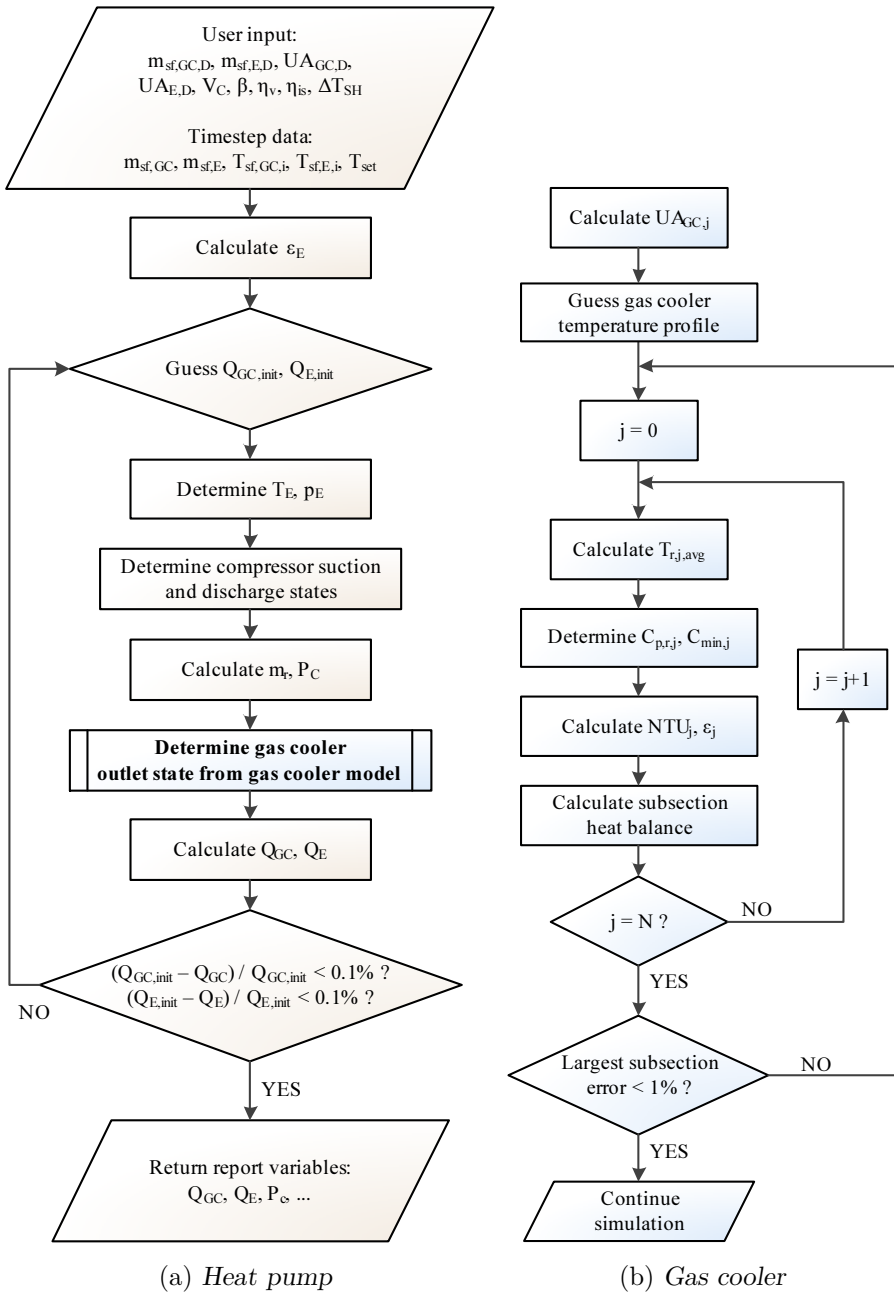


Figure 4.4: Calculation steps for the heat pump model and the gas cooler model

## 4.2 Implementation into EnergyPlus

EnergyPlus is an open-source whole building energy simulation program written in Fortran 90. It is developed by the U.S. Department of Energy and aims to integrate all aspects of the simulation by coupling the building energy supply systems and loads with the thermal response of the building. It is purely a simulation engine due to the lack of a user interface, although third-party interfaces exist. All inputs and outputs are in plain text format, and there is a vast number of input parameters available for a very detailed description of the building floor plan and envelope, the building's HVAC system and its usage patterns. Interaction between the energy supply systems and the building loads is modeled by means of system loops. A loop is made up of two half-loops connected to each other. The supply equipment (e.g. a boiler) is placed on the *plant side* of the loop, while the demand equipment (e.g. a heating coil) is placed on the *demand side*. Figure 4.5 shows an overview of the EnergyPlus system manager and the loop concept.

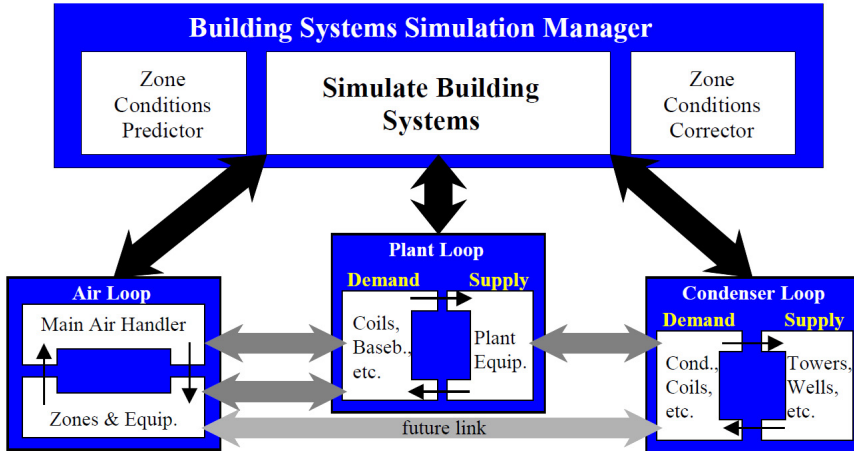


Figure 4.5: Overview of the connections between the main HVAC simulation loops and half loops in the EnergyPlus systems manager (EnergyPlus, 2012)

An existing model of a *conventional* heat pump in EnergyPlus is developed by Jin (2002), where a parameter estimation procedure is employed in order to determine the necessary model input parameters from heat pump catalog data. The original EnergyPlus module for this heat pump

model with the modifications made by Murugappan (2002) provided a basis for the new transcritical model. In this way the existing subroutines for input and output handling, initialization and more could to some extent be reused. In this model the secondary fluid loops of both the gas cooler and evaporator are liquid loops. An air-source heat pump was therefore modeled by means of a glycol mix loop on the evaporator side containing a fluid heater like shown in Figure 4.6. In this way the glycol mix entering the evaporator held the same temperature as the outdoor air at all times, making the heat pump performance resemble that of an air-source heat pump. Because of the way the system loops and component calling structure and order in EnergyPlus works, modeling of bipartite and tripartite gas cooler system like those described in Chapter 2.3 (i.e. with more than one component on the load side of the heat pump) could present some challenges.

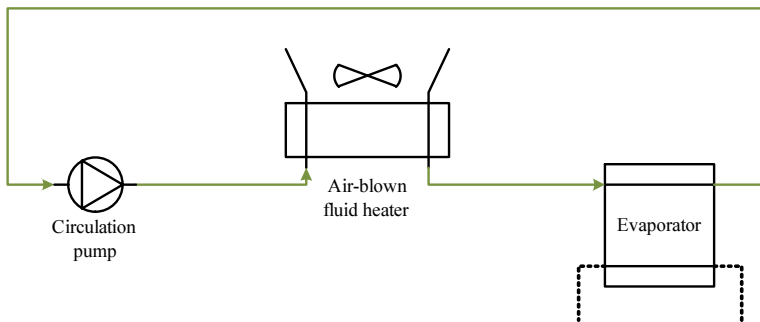


Figure 4.6: *Illustration of the glycol mix loop on the evaporator side as modeled in EnergyPlus*

As entropy data for  $\text{CO}_2$  were needed for the compressor component of the model, a new set of  $\text{CO}_2$  thermodynamic properties data based on the correlations of Span and Wagner (1996) were calculated using RefProp (Lemmon et al., 2007) and FluidProp (Colonna and van der Stelt, 2004) and added to the the EnergyPlus input files. Also, the EnergyPlus fluid properties module `FluidProperties.f90` was extended with an entropy retrieval function which, given temperature and pressure, retrieves the entropy by interpolation. Data were in the range of  $-50^\circ\text{C}$  to  $+30.9^\circ\text{C}$  for the saturated region and from  $-40^\circ\text{C}$  to  $+180^\circ\text{C}$  and 10 bar to 120 bar for the superheated region. Particular care was taken to the large



variations close to the critical point by using smaller temperature and pressure steps in this region. To avoid large interpolation errors around the critical point the heat pump was also restricted to never operate at discharge pressures lower than 75 bar. An upper limit of 120 bar was also set in order to avoid excessive discharge temperatures from the compressor. Calculated property data converted into EnergyPlus input format can be found in the attached file `R744Properties.txt`.

### 4.3 Preliminary study of model

An assessment of the peak heating load of the building described in Chapter 5 was necessary in order to determine appropriate input parameters for the heat pump. A simulation of a reference model with direct electric heating was therefore performed in EnergyPlus with the results described in Chapter 6.1. Based on these results it was decided to implement a heat pump with a heating capacity of 9 kW for the subsequent simulations giving a heating load coverage factor of a little less than 60%.

A preliminary study of the heat pump model was then carried out using Microsoft Excel (`HPModel.xlsx`) in order to determine the optimal component dimensions and control of the heat pump in the subsequent building simulations. As heat pump capacity drops with decreasing outdoor temperature, it was decided that the unit should be able to deliver 9 kW at an outdoor temperature of  $-7^{\circ}\text{C}$ . The temperature was chosen based on the requirements for a similar prototype air-to-water heat pump described in the technical report by Stene and Skiple (2007). All calculations within the current section were done with the assumption of the input values shown in Table 4.1.

	Symbol	Value
Volumetric efficiency	$\eta_{vol}$	0.7
Isentropic efficiency	$\eta_{is}$	0.55
Heat loss factor	$\beta$	0.1
Suction gas superheat	$\Delta T_{SH}$	$5^{\circ}\text{C}$
Gas cooler subsections	N	20

Table 4.1: *Constant values assumed for parametric study of heat pump model*

An increased gas cooler CO<sub>2</sub> outlet temperature leads to a higher outlet enthalpy and with that a higher evaporator inlet enthalpy. This gives a lower VRC (Equation 2.1) and consequently a higher necessary displacement volume for a given rate of heat transfer. The compressor displacement volume was therefore calculated for the highest CO<sub>2</sub> outlet temperature, which occurred in space heating mode when the return temperature was 30°C.

The heat pump performance was investigated for different combinations of UA-values and gas cooler pressures giving a heat capacity of 9 kW at -7°C outdoor temperature. Figure 4.7 shows the variation of COP with varying gas cooler UA-value for different gas cooler pressures when the secondary fluid is heated from 30 to 35°C and the evaporator UA-value is 2000 W/K. Results showed that there was a relatively small performance gain with increased evaporator UA-values above 2000 W/K. For further study it was therefore decided to assume this value, but in reality one would also have to consider the costs of an increased heat exchanger size versus the savings due to better performance. Results for other evaporator UA-values can be found in Appendix B.

In Figure 4.7 two points which were considered good options are marked. These are for gas cooler UA-values of 800 W/K and 1300 W/K at gas cooler pressures of 90 bar and 85 bar respectively. It is clear that increasing the gas cooler UA-value above these values at the given pressures did not significantly increase the COP. This was because the CO<sub>2</sub> outlet temperature approached the secondary fluid inlet temperature and therefore further cooling of the CO<sub>2</sub> would not be possible (ref. Chapter 2.1.2). It is further seen that a gas cooler UA-value of 1300 W/K at 85 bar gave a slightly higher COP under the simulated conditions than a gas cooler value of 800 W/K at 90 bar. Figure 4.8 suggests that a small performance increase could also be expected when heating the secondary fluid from 7 to 65°C by choosing the higher UA-value. It was therefore decided on a gas cooler value of 1300 W/K which resulted in a necessary compressor displacement of approximately 2.9 m<sup>3</sup>/hr at the specified conditions.

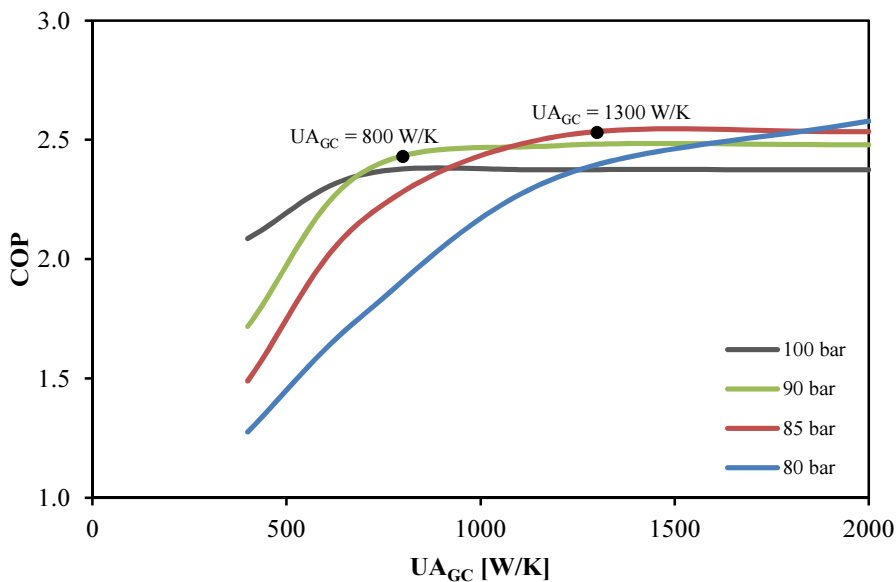


Figure 4.7: COP vs. gas cooler UA-value at different gas cooler pressures. Secondary fluid heated from 30 to 35°C, evaporator UA-value is 2000 W/K.

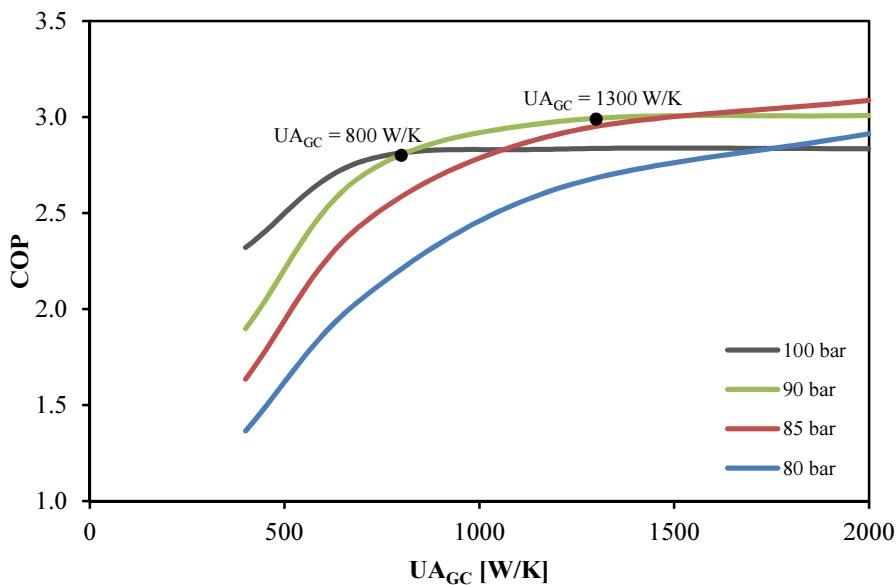


Figure 4.8: COP vs. gas cooler UA-value at different gas cooler pressures. Secondary fluid heated from 7 to 65°C, evaporator UA-value is 2000 W/K.

The heat pump performance was further analyzed over the ranges of operation shown in Table 4.2. For this analysis the outdoor air temperature was held constant at 7°C which was the yearly average temperature at the location of the building of interest.

	Variable	Range
Water inlet temperature	$T_{sf,GC,in}$	10°C to 30°C
Water setpoint	$T_{set}$	35°C to 65°C

Table 4.2: *Temperature ranges for which the optimal pressure was calculated*

It was assumed a linear relation between the optimal gas cooler pressure and the secondary fluid gas cooler inlet temperature when the setpoint temperature was held constant similar to the approach of Chen and Gu (2005). Similarly, a linear relation between the optimal gas cooler pressure and the secondary fluid setpoint temperature (i.e. the *outlet* temperature from the gas cooler) was assumed when the inlet temperature was held constant. The proposed relation for control of the gas cooler pressure was then determined by method of least squares as:

$$p_{GC} = 0.00504T_{set}T_{sf,GC,in} + 0.773T_{set} + 0.269T_{sf,GC,in} + 41.3 \quad (4.13)$$

In Equation 4.13 the temperatures are in [°C] while the pressure is given in [bar]. Results used for determining this relation can be found in Appendix C and `HPModel.xlsx`. The relation was hard-coded into EnergyPlus, but the possibility to specify the coefficients in the EnergyPlus input file should ideally be implemented as they could differ for a heat pump with different specifications. A comparison between the pressure predicted from Equation 4.13 and the actual optimal pressure is shown in Figure 4.9. It can be seen that the predicted pressure generally stayed within  $\pm 5\%$  of the optimal pressure in the temperature ranges of interest. Even though the optimal pressure dependency on evaporation temperature is supposedly low (Chapter 3.7) the deviation will expectedly be larger when operating at varying outdoor temperature.

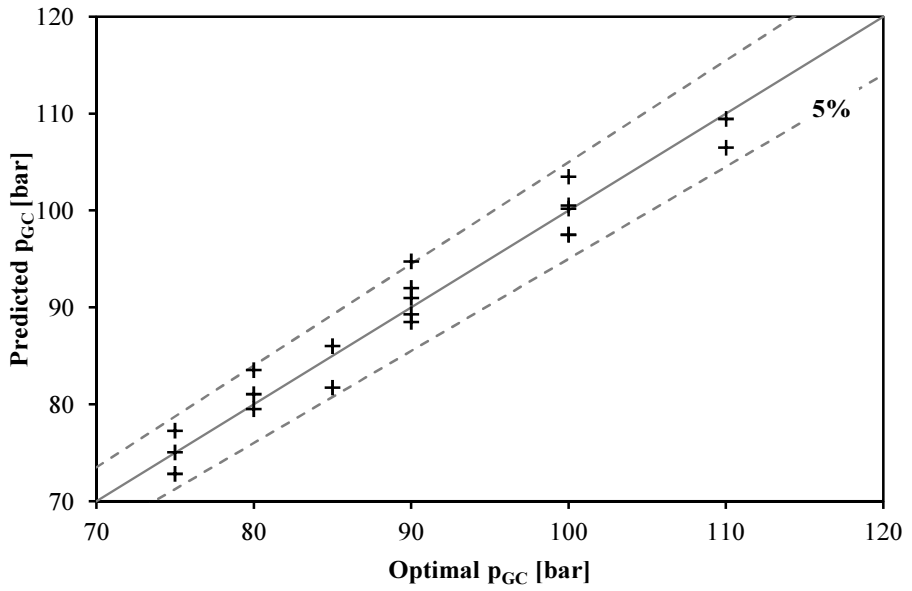


Figure 4.9: Comparison of the pressure predicted by Equation 4.13 and the actual optimal pressure in the range tested at constant outdoor temperature of 7°C.



## 5 Building and simulation inputs

### 5.1 Building overview

For simulations in EnergyPlus a three-story residential building was modeled in Trimble SketchUp. It was based on a building used in previous simulations and consisted of three apartments, one in each story. Building geometry and dimensions were as shown in Figure 5.1. The total building area was 450 m<sup>2</sup> split evenly between the three apartments. The building location was set to Oslo, Norway, using the IWEC<sup>6</sup> hourly weather data for Oslo/Fornebu. With the values given in Table 5.1, the building envelope met the criteria for a "Low energy building, class 1" as specified in NS3700 (2010). The building had a window-to-wall ratio of 13.4%.

	Model	NS 3700
Exterior walls	0.16	$\leq 0.18$
Windows	1.2	$\leq 1.2$
Roof	0.11	$\leq 0.13$
Base floor	0.15	$\leq 0.15$

Table 5.1: *Building envelope U-values [W/(m<sup>2</sup>-K)]*

The air infiltration rate was set to 0.5 ACH<sup>7</sup>. The ventilation system was a balanced system with sensible and latent heat recovery, with an assumed effectiveness of 80% at full air flow for the heat recovery system. Ventilation air flow rates and internal gains from people, lighting and electrical equipment were all based on the recommended values for energy demand analysis found in NS3700 (2010). Each apartment was assumed to have four occupants, and was split into three thermal zones; Hallway, living room and bathroom with air temperature setpoints of 20°C, 21°C and 21°C respectively. The apartments had the floor plan shown in Figure 5.2.

---

<sup>6</sup>International Weather for Energy Calculation; Hourly weather data supplied by ASHRAE

<sup>7</sup>Air Changes per Hour

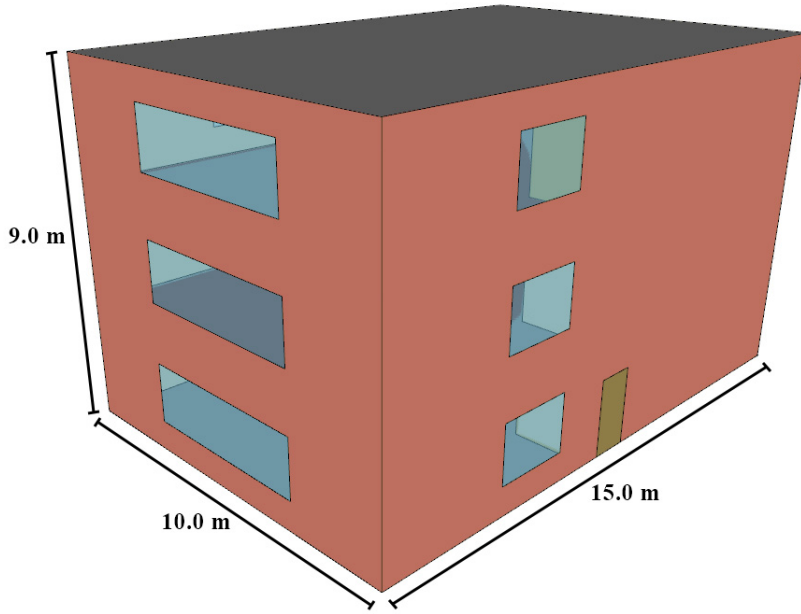


Figure 5.1: Geometry and dimensions of the building used for simulations

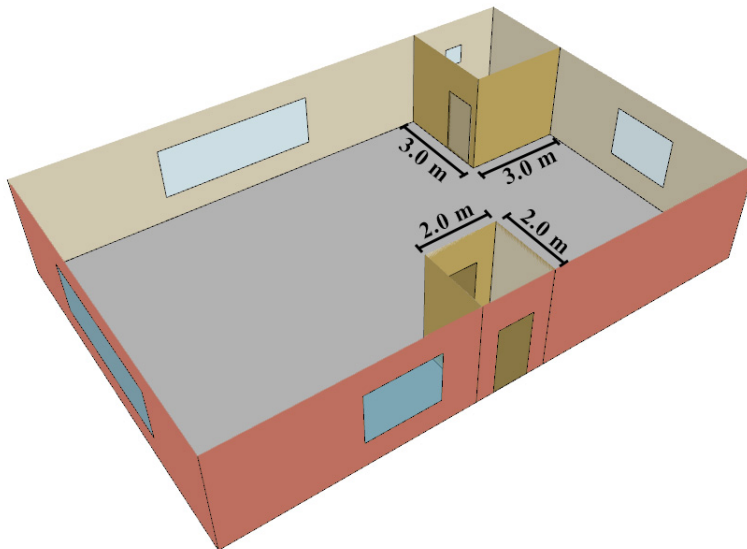


Figure 5.2: Floor plan of one apartment. All apartments had identical floor plans.



## 5.2 Domestic hot water and hydronic heating system

It was desired to model a system consisting of a tripartite gas cooler like the one presented in Chapter 2.3. However, in EnergyPlus the heat pump could only be connected to one single loop on the gas cooler side. The system was therefore modeled with an intermediate water loop containing three ideal heat exchanger as shown in Figure 5.3. This would not be entirely realistic because the water in the intermediate loop would in this case flow through the same gas cooler in DHW mode as in space heating mode. In reality there would be separate flows through separate gas coolers in the two modes.

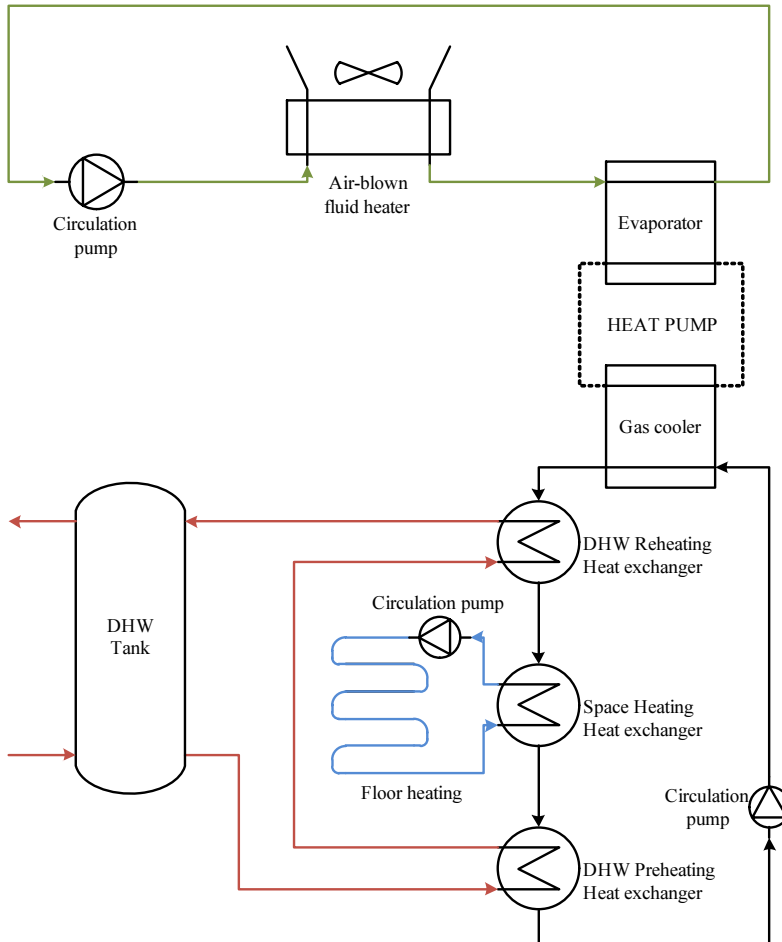


Figure 5.3: Illustration of EnergyPlus system

A variable-flow hydronic underfloor heating system was chosen for space heating. The system was dimensioned for relatively low supply and return temperatures of 35°C and 30°C respectively. This should benefit the heat pump performance when operating in space heating mode as discussed in Chapter 2.3.2. An additional 9 kW of supplementary electric heating was installed in order to cover the peak load.

The DHW tank was cylindrical with a height of 2.0 m and a volume of 500 litres. This gave a relatively small diameter-to-height ratio of 0.28 which should help reducing conduction and mixing inside the tank. The tank was split into ten nodes of equal height for modeling thermal stratification of the water as illustrated in Figure 5.4. The setpoint of the hot water was 65°C in all the cases studied. A 5 kW electric heating element was placed near the top of the tank (node 9) for supplementary heating when the heat pump was not able to meet the demand. The cut-in temperature for the supplementary heating was 50°C. Thermal losses from the tank was set to 0.9 W/(m<sup>2</sup>-K).

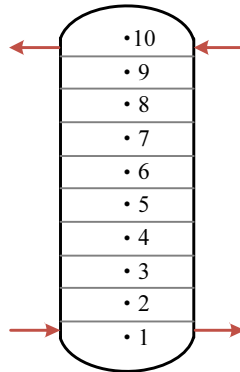


Figure 5.4: *Illustration of the DHW tank as modeled in EnergyPlus*

In an actual building tap water are drawn irregularly and over very short time periods which is hard to model realistically in a simulation program like EnergyPlus. The consumption of DHW was therefore assumed to follow a simple schedule resembling a typical pattern for a residential building with the use of showers in the morning and cooking/showers in the afternoon and evening. Tap water draw rates were set to 70% of the maximum draw rate from 06:00 to 08:00 and 60% of the maximum draw

rate from 18:00 to 21:00. The maximum draw rate were set so that the recommended value in NS3700 (2010) of 29.8 kWh/(m<sup>2</sup>-year) for DHW demand was matched as closely as possible. It was assumed that water from the DHW tank was mixed with cold water from the mains giving a tap water temperature of 40°C. Cold water from the mains was assumed to have a temperature of 7°C. In reality this temperature would vary throughout the year.

### 5.3 Case study overview

Four different cases were chosen for simulations in EnergyPlus. The first was a reference case while the other three incorporated a heat pump in the energy supply system.

- **Reference case:** In this direct electric reference model all heating demands were met by means of direct electrical heating with an assumed efficiency of 100% and a total capacity of 18 kW. The capacity was distributed as 4.5, 0.75 and 0.75 kW for each living room, bathroom and hallway respectively. The DHW tank was of the same dimensions as described in Chapter 5.2, but had a 7 kW heating element. Inputs were otherwise as described in Chapter 5.1.
- **Case A:** In this heat pump "base case" a heat pump was included as shown in Figure 5.3. Heat pump input parameters were as described in Chapter 4.3 with the exception of the number of gas cooler subsections which was raised to 50. Other inputs were as described in Chapters 5.1 and 5.2. This was thought to represent use of the building under normal conditions.
- **Case B:** Here the DHW consumption was set 50% higher than in Case A. As the draw schedule stayed the same, this gave a higher peak tap water draw rate.
- **Case C:** In this case a reduction of the indoor air temperature during night-time was introduced. The air temperature setpoint was lowered to 18°C in all rooms every night between 22:00 and 06:00. The DHW consumption was the same as in Case A.



## 6 Results

This chapter starts with an assessment of the building peak load and energy consumption. It then continues with a presentation and comparison of the energy use in each of the cases studied followed by a discussion of the heat pump performance in each separate case. All simulations in this section were run over the course of one full year. Simulations were run with sub-hourly timesteps of 15 minutes and the resulting data were then reduced to hourly data.

### 6.1 Building peak load and energy consumption

In the case of the direct electric reference model the annual end-use energy consumption was found to be 40 979 kWh which for this building equaled 91.1 kWh/(m<sup>2</sup>-year). A total of 31 031 kWh went to heating. The monthly distribution of energy end-use was as shown in Figure 6.1. The category labeled "El. specific" comprised loads that could not be met by other means than electricity and included lighting, electrical appliances and pump/fan work. Space heating was at a maximum of 3 923 kWh in January and very low or not present at all in the months of May to September. The domestic hot water energy consumption stayed relatively constant at about 1 100 kWh/month throughout the year, and the el. specific energy consumption saw very slight variations between 780 and 890 kWh/month. The latter was due to increased work by the ventilation air heat recovery system during winter months. The heating load duration curve is shown in Figure 6.2. The total peak load for the building was found to be 17.4 kW, with the peak heating load being 15.7 kW. The peak heating load provided the basis for the dimensioning of the heat pump as described in Chapter 4.3.

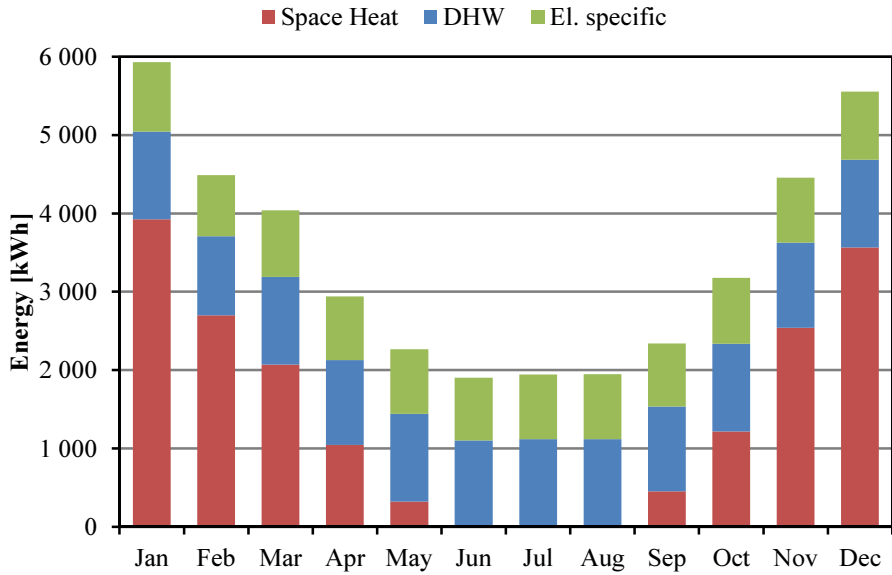


Figure 6.1: Monthly energy end-use for electric reference model

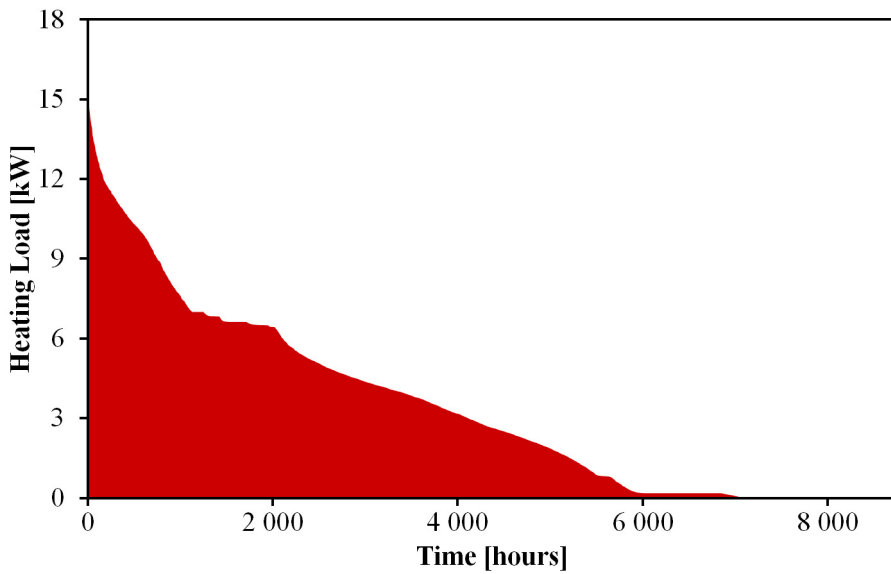


Figure 6.2: Heating load duration curve for electric reference model

## 6.2 Initial comparison of energy use

Figure 6.3 shows a comparison of the total site energy consumption. These numbers include power input to the heat pump, supplementary electrical heating and all electricity for lighting, equipment, pumps and fans. The energy consumption was reduced from 40 979 kWh in the reference case to 24 144 kWh in the base case which corresponded to a yearly reduction of 16 835 kWh. In the cases of increased DHW usage and night-time temperature reduction the consumption was 25 230 kWh and 24 002 kWh respectively. The energy end-use was distributed as shown in Figure 6.4. The specific energy end-use increased in all three heat pump cases from 91.1 kWh/(m<sup>2</sup>-year) in the reference case to 96.8, 106.7 and 93.5 kWh/(m<sup>2</sup>-year) respectively. This was mainly a consequence of the additional pump work needed for the heat pump system. In Case B the 50% increase in DHW consumption obviously also contributed to the increased end-use.

In Figure 6.5 the total heating demand is divided into demand for space heating and for DHW. Each is further divided into the demand covered by the heat pump and the demand covered by direct electric heating. The DHW demand makes up from 42% to 52% of the total heating demand in the different cases. This is quite high, which is to be expected with the reduced space heating demand of a low energy building. It can further be seen that the heat pump covered a very high percentage of the total heating demand, ranging from 93.0% in Case C to 96.2% in Case A with Case B inbetween at 95.4%. This could be a result of the relatively high peak heating load coverage of 57%, which was in the upper part of the suggested range (Chapter 2.4), and might suggest that a lower load coverage would have been optimal.

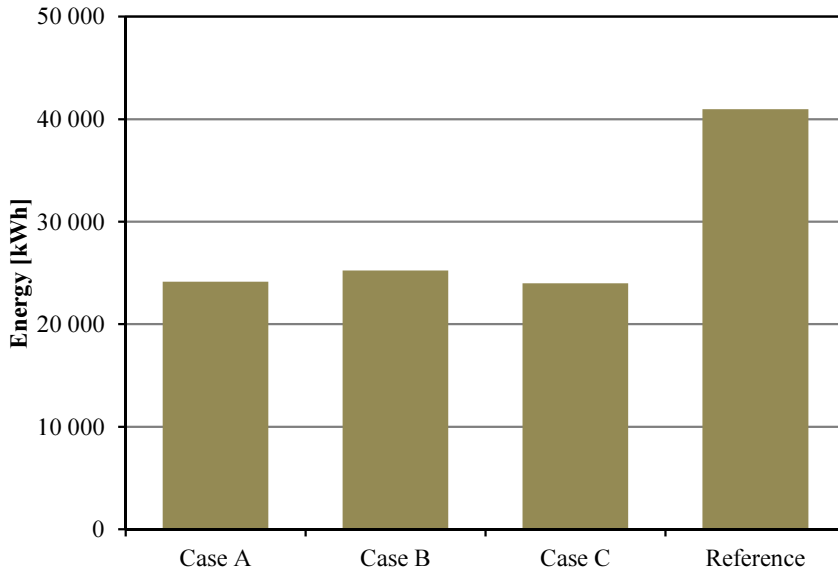


Figure 6.3: Comparison of the total site energy consumption in each of the cases studied including space heating, DHW and el.specific use.

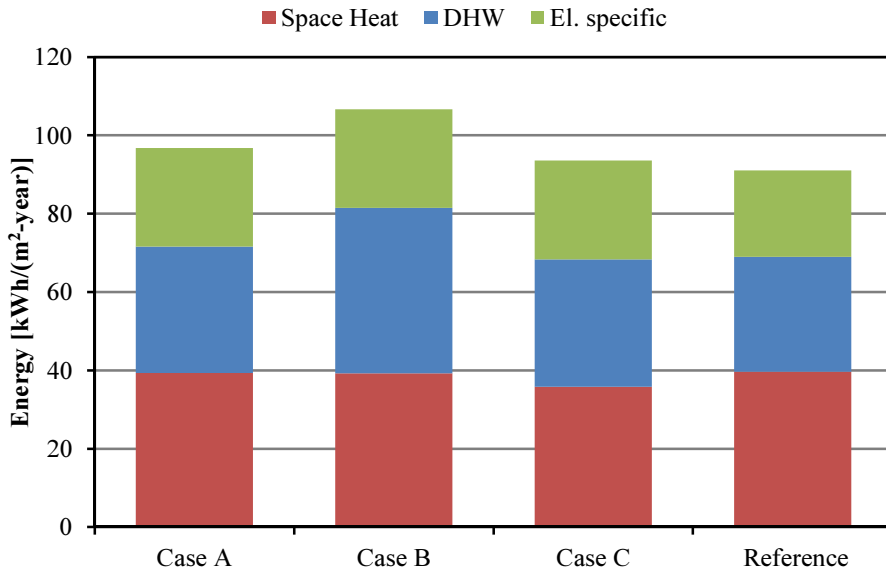


Figure 6.4: Comparison of the specific energy end-use distribution in each of the cases studied.



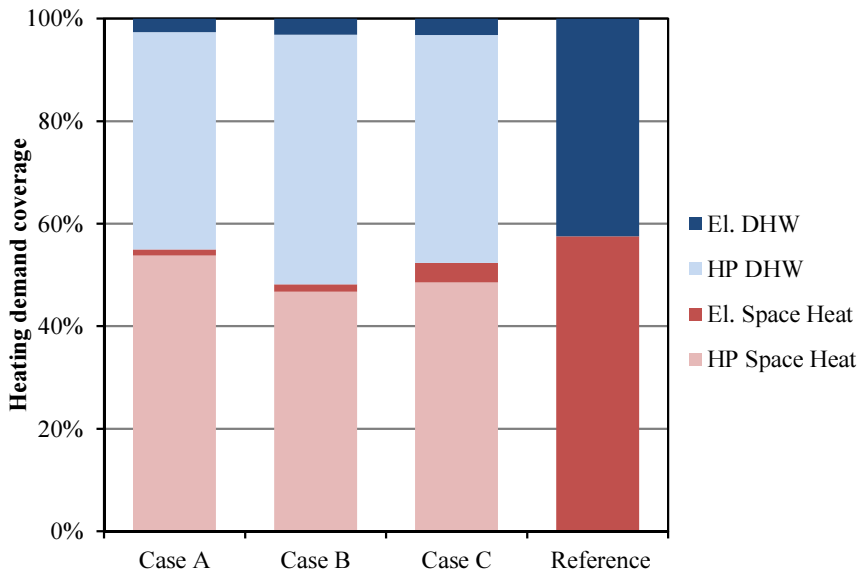


Figure 6.5: Comparison of heat pump coverage and supplementary system coverage of the heating demand in each of the cases studied.

### 6.3 Case A: Base case

Figure 6.6 shows the heating load duration curve for the heat pump base case. It is apparent that the curve is steeper than that of the electric reference case in Figure 6.2. This is because the intermittent operation of the heat pump prevented operation at very low loads. The heat pump therefore operated less frequently, but at a higher capacity, than it would with continuous operation. The highest loads occurred when the heat pump supplied heat for both space heating and DHW simultaneously in combined mode. Supplementary electric heating was therefore almost exclusively only necessary in this operating mode. The duration curve also reveals that the heat pump often operated at a higher capacity than the design capacity of 9 kW. This means that the operating conditions often were more favorable than the design conditions, and this could support the earlier statement about the installed heat pump capacity being higher than optimal. The relatively high equivalent operating time of 3 444 hours could however indicate a good utilization of the heat pump.

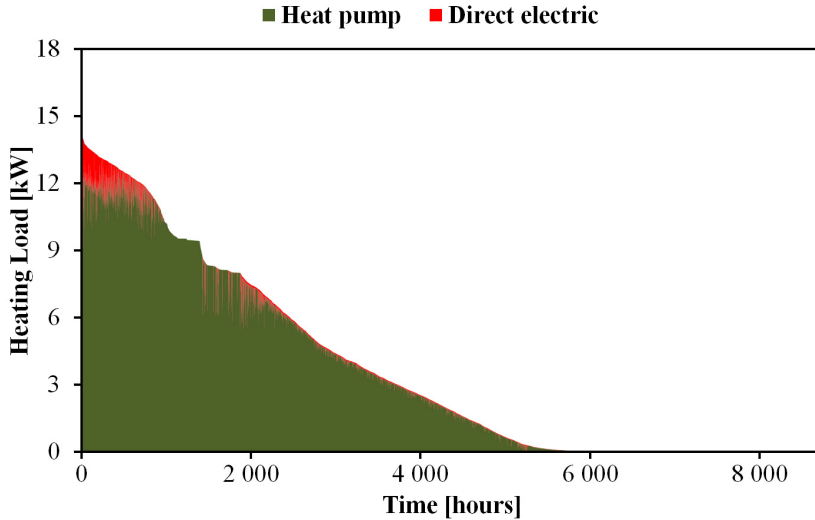


Figure 6.6: Case A: Heating load duration curve

Figure 6.7 shows how the COP varied with outdoor air temperature. Here it is clear that the performance in combined mode and DHW-only mode suffered badly. The average COP of 2.52 in DHW-only mode was lower than the average COP of 2.66 in space heating-only mode, which is the opposite of what would be expected. The reason for this is that the heat pump operates in DHW-only mode mainly during the summer season when there is no space heating demand, and it is during summer season the drawbacks of the single-speed compressor discussed in Chapter 2.2 become most apparent. At high outdoor air temperatures the heat pump capacity was significantly larger than the DHW heating demand, leading to high CO<sub>2</sub> gas cooler outlet temperatures because of insufficient cooling of the gas. The increasing heat pump performance due to high outdoor temperatures were therefore offset by the large mismatch between heating capacity and building demand. Under these circumstances the use of a variable-speed compressor would expectedly increase the performance.

Calculations from the MS Excel model used for preliminary studies indicated that a COP of 3.50 to 3.80 could be achievable at outdoor temperatures between 10 and 20°C for the heat pump studied. This was with the assumption that the temperature difference between the gas cooler water inlet and CO<sub>2</sub> outlet could be reduced to 3°C by regulation of the

capacity. Assuming an average COP of 3.60 from the middle of May to the middle of September, additional energy savings were estimated to 662 kWh which would increase the heat pump SPF to 2.83 and the system SPF to 2.65. As pointed out in Chapter 2.4 the relative energy savings from such a slight increase in SPF would not be huge. Even with a large increase in COP during summer season the actual savings would be moderate due to the fact that the heating demand during summer months made up a relatively small amount of the total yearly heating demand.

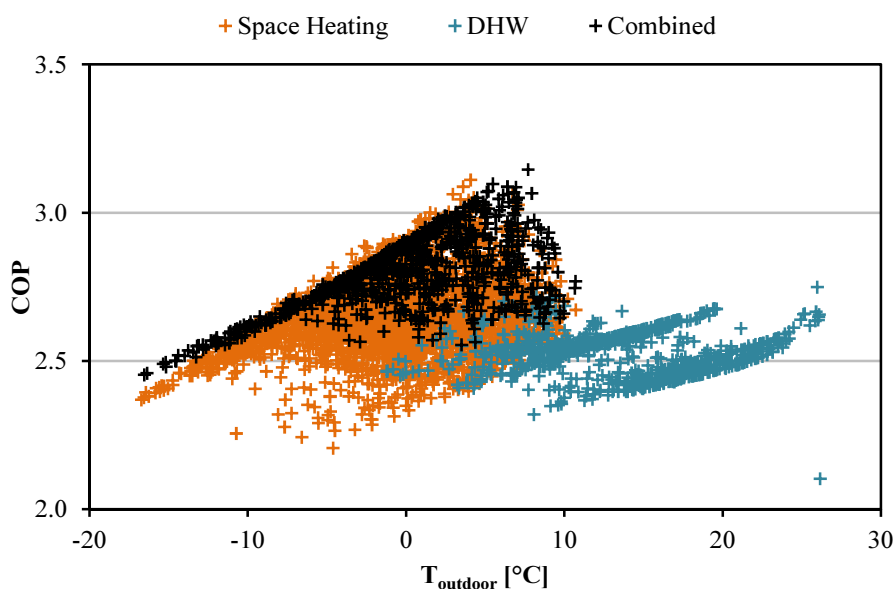


Figure 6.7: Case A: Variation of COP with outdoor air temperature for the different heating modes.

#### 6.4 Case B: Increased consumption of domestic hot water

With a 50% increase in DHW consumption the total energy end-use increased to 106.7 kWh/(m<sup>2</sup>-year) corresponding to a 10.2% increase compared to Case A. In this case the DHW heating demand made up more than half of the total heating demand with a DHW ratio of about 52% as shown in Figure 6.5. The heating demand coverage stayed virtually the same as in Case A, supporting that the installed capacity could indeed

be too high in Case A. The heat pump SPF and overall system SPF increased to 2.87 and 2.64 respectively.

The duration curve in Figure 6.8 can roughly be split into three parts. The leftmost part of the curve, from hour zero to around hour 1100, consists mostly of the times when the heat pump operated in combined mode. This is when most of the demand for supplementary heating occurred. The relatively flat part from hour 1100 to around hour 1800 mainly represents the times when the heat pump operated in DHW-only mode, i.e. the summer season. It can be seen that supplementary heating was generally not needed during summer season even with the increased DHW consumption. The heat pump still had the capacity to cover the DHW heating demand due to the favorable operating conditions caused by high outdoor temperatures. The performance in space heating-only mode was basically the same as in Case A.

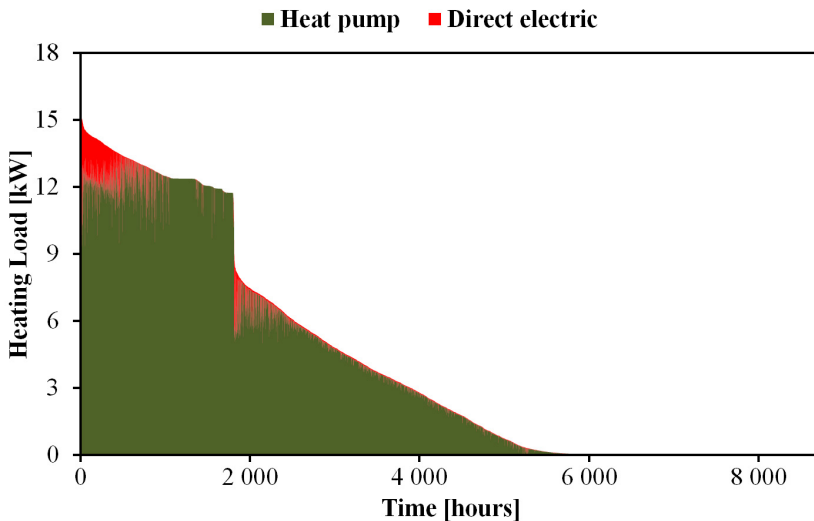


Figure 6.8: Case B: Heating load duration curve

Because of the increased DHW consumption there was a better match between building load and heat pump capacity during summer season than in Case A. This shows clearly in Figure 6.9 where the COP in DHW-only mode was on average considerably higher than in Case A (Figure 6.7). The COP also increased in combined mode for the same reason, especially at high outdoor temperatures. Performance in this

case was more in line with what would be expected from a CO<sub>2</sub> heat pump, especially in combined mode where a higher COP was achieved in general.

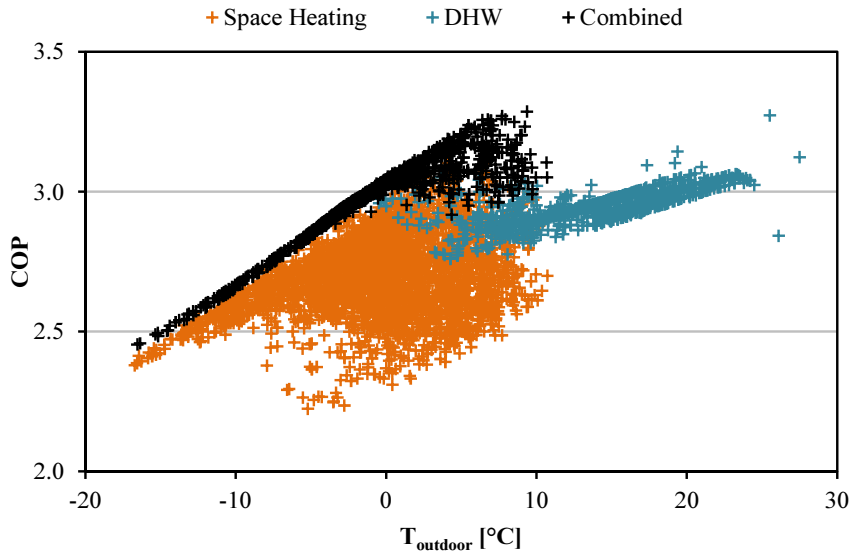


Figure 6.9: Case B: Variation of COP with outdoor air temperature for the different heating modes.

## 6.5 Case C: Reduced indoor temperature during night-time

In Figures 6.10 and 6.11 the variation of indoor air temperature in the living room of the first floor apartment is shown together with the variation of the heat pump heating load for Case A and Case C. These are for a typical winter day (January 22). Because of the low transmission losses through the building envelope it took relatively long time before the temperature reduction came into effect. As can be seen in Figure 6.11 the indoor temperature did not reach the reduced value until around 03:00. With space heating commencing around 05:00 the effective time period of temperature reduction became rather short. This could suggest that night-time temperature reduction is a less effective energy-saving measure in the case of a low energy building as compared to a regular building.

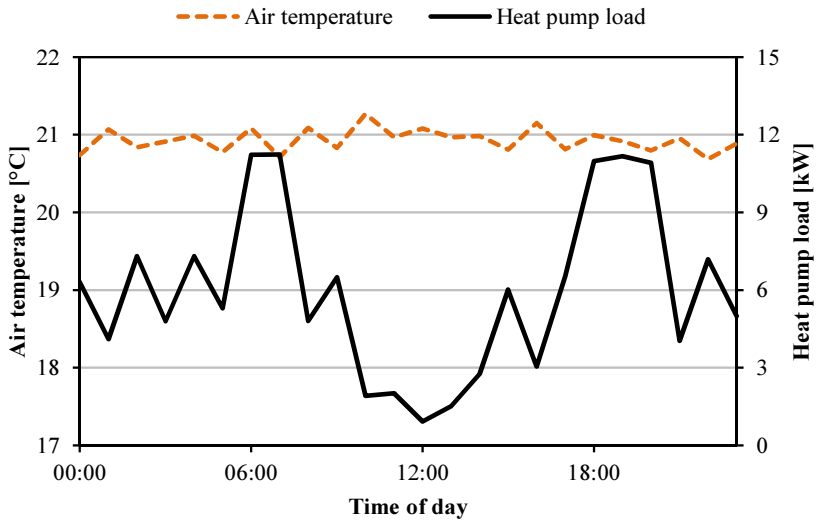


Figure 6.10: Case A: Variation of first floor living room air temperature and heat pump heating load *without* night-time temperature reduction over the course of a typical winter day.

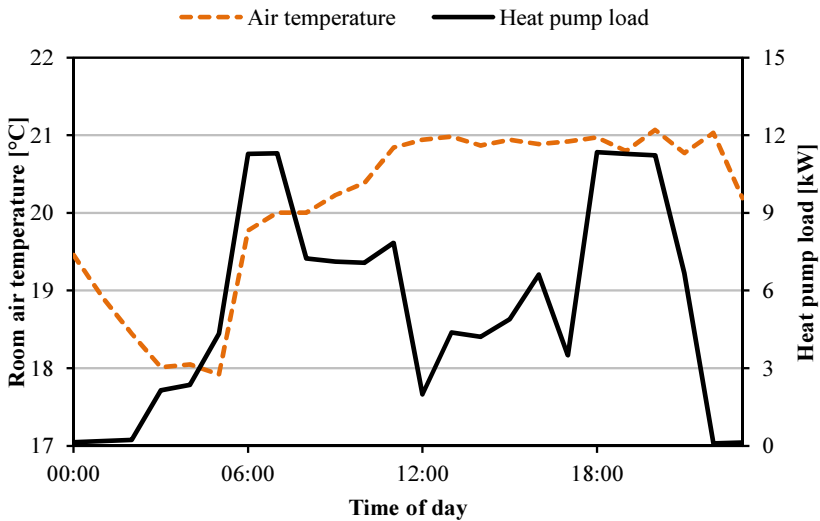


Figure 6.11: Case C: Variation of first floor living room air temperature and heat pump heating load *with* night-time temperature reduction over the course of a typical winter day.

The 3°C reduction of indoor temperature during night-time resulted in the duration curve shown in Figure 6.12. The peak load was noticeably higher than in Case A. This was because of the large heating demand when heating the building in the morning. In Figures 6.10 and 6.11 it can be seen that the increased space heating demand during the morning hours due to the night-time temperature reduction coincided with the large DHW demand in the morning. This resulted in an increased demand for supplementary direct electric heating. Also, because of the coinciding space heating and DHW demands it often took considerable time before the indoor temperature reached the desired setpoint value. Thermal discomfort could therefore be an undesirable side-effect for occupants in the case of night-time temperature reduction. It could be avoided by increased use of supplementary heating, but this would give a lower system SPF and possibly lead to a larger total site energy consumption than in Case A.

From Table 6.1 it can be seen that the heat pump SPF increased while the overall system SPF decreased compared to Case A. While the heat pump achieved a higher SPF because of less frequent operation at generally higher loads, the system SPF was lower due to the additional need for supplemental heating. Consequently the site energy savings in Case C as compared to Case A were miniscule at 142 kWh/year or about 0.6%. Figure 6.13 shows that the COP in DHW-only mode and combined mode was comparable to that of Case A. The high space heating load caused by reheating of the building in the morning hours resulted in a somewhat increased performance in space heating mode, but again this had a very little effect on energy savings. Based on these results a reduction of the night-time indoor temperature would not be recommended.

	Heat Pump SPF	System SPF	$\tau$ [h]
Case A	2.67	2.51	3 444
Case B	2.87	2.64	3 887
Case C	2.72	2.43	3 180

Table 6.1: *Summary of simulation results for each case*

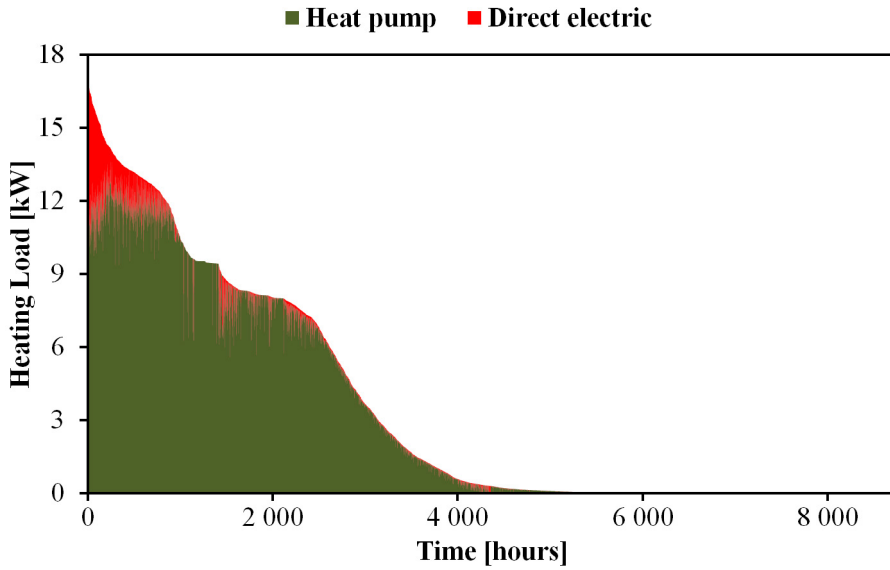


Figure 6.12: Case C: Heating load duration curve

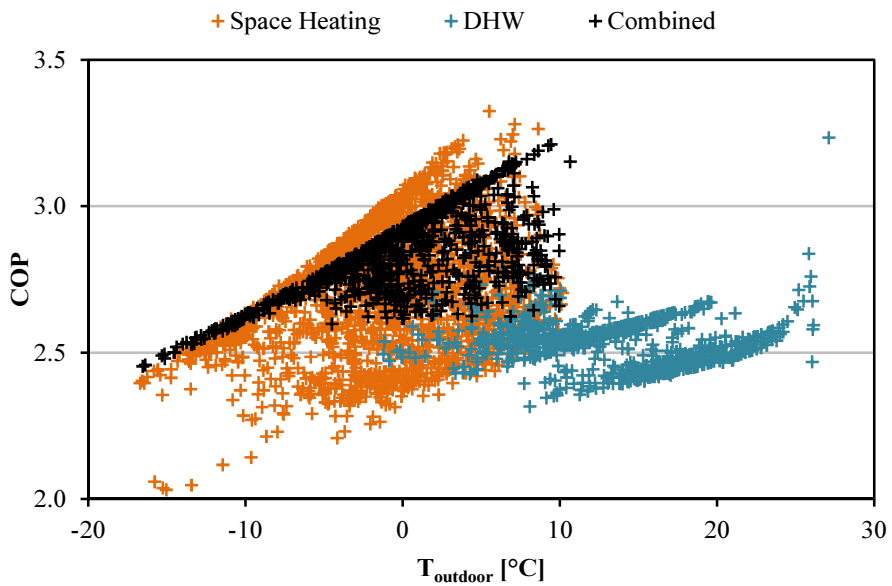


Figure 6.13: Case C: Variation of COP with outdoor air temperature for the different heating modes.



## 7 Conclusions and suggestions for further work

A transcritical heat pump model was developed and implemented into EnergyPlus. The model was based on earlier developed models described in Chapter 3. However the fact that the model was not validated against experimental data should be taken into account when evaluating the simulation results.

Challenges related to the heat pump model included finding an appropriate balance between the level of complexity of the model and simplifications needed in order to implement the model into an existing energy simulation program. Making the model work with the existing modules in EnergyPlus required lots of trials and debugging, and there were especially difficulties related to the implementation of capacity controls for variable-capacity operation. Consequently only single-speed operation was implemented. There were also some doubts regarding how realistically the system modeled in EnergyPlus represented the systems described in Chapter 2.3 as some workarounds had to be made in order to get the EnergyPlus model to work.

Simulations of the building were run in three different cases representing different operating conditions for the heat pump. In the "base case" the heat pump achieved a SPF of 2.67 while the overall system SPF was 2.51. With an increased demand for domestic hot water both heat pump and overall system SPF increased reaching 2.87 and 2.64 respectively. This was mainly due to the better match between heat pump capacity and building load at medium to high outdoor temperatures. The heat pump was able to cover more than 90% of the heating demand even in the case of increased DHW consumption which could indicate that a lower installed capacity would be optimal. It nevertheless demonstrated the suitability of CO<sub>2</sub> heat pumps when there is a high relative demand for domestic hot water. In the case of reduced night-time indoor temperature the heat pump SPF increased to 2.72. However the overall system SPF decreased due to the increased need for supplementary heating. In this case the energy savings were negligibly small, and there was a risk of decreased indoor thermal comfort. A reduction of night-time indoor temperature in the building of interest would therefore not be recommended.

The simulation results indicated that the system was prone to performance degradation due to mismatch between load and capacity in all the tested cases, especially during summer months. Based on this a variable speed control of the compressor would be recommended. The energy savings were however estimated to be moderate, and this would have to be weighed against possibly increased investment costs.

The following are suggestions for further work:

- Validation of the heat pump model in order to establish the reliability of simulation results.
- Development of a parameter estimation procedure similar to that which already exists for conventional heat pumps in EnergyPlus. This would be a great aid in determining the correct input parameters for a specific heat pump from catalog data.
- Extension of the heat pump model by incorporating variable capacity controls and compressor efficiencies based on curve inputs rather than constant values.
- Due to time restrictions the heat pump simulations were limited to only three different cases in EnergyPlus, which was less than desired. Further investigation of optimal installed capacity could be made. A performance comparison of the transcritical heat pump and a conventional heat pump in the same building under the same conditions would also be informative.

## References

- Arora, R. C. (2010).** *Refrigeration and Air Conditioning*. PHI Learning.
- ASHRAE (2005).** “Thermophysical properties of refrigerants.” In “ASHRAE Handbook - Fundamentals (SI),” .
- Austin, B. T. and Sumathy, K. (2011).** “Transcritical carbon dioxide heat pump systems: A review.” *Renewable and Sustainable Energy Reviews*, 15(8): 4013–4029.
- Brown, J. S. and Domanski, P. A. (2000).** “Semi-Theoretical Simulation Model for a Transcritical Carbon Dioxide Mobile A/C System.” In “SAE 2000 World Congress,” Detroit, Michigan, United States.
- Cecchinato, L., Corradi, M., and Minetto, S. (2011).** “A simplified method to evaluate the energy performance of CO<sub>2</sub> heat pump units.” *International Journal of Thermal Sciences*, 50(12): 2483–2495.
- Chen, Y. and Gu, J. (2005).** “The optimum high pressure for CO<sub>2</sub> transcritical refrigeration systems with internal heat exchangers.” *International Journal of Refrigeration*, 28(8): 1238–1249.
- Colonna, P. and van der Stelt, T. (2004).** “FluidProp: a program for the estimation of thermo physical properties of fluids.”
- Dang, C., Iino, K., Fukuoka, K., et al. (2007).** “Effect of lubricating oil on cooling heat transfer of supercritical carbon dioxide.” *International Journal of Refrigeration*, 30(4): 724–731.
- Dokka, T. H. and Hermstad, K. (2006).** *Energieffektive boliger for fremtiden - En håndbok for planlegging av passivhus og lavenergiboliger*. IEA SHC Task 28/ECBCS Annex 38: Sustainable Solar Housing. Husbanken/Sintef Byggforsk/NTNU.
- Fernandez, N., Hwang, Y., and Radermacher, R. (2010).** “Comparison of CO<sub>2</sub> heat pump water heater performance with baseline cycle and two high COP cycles.” *International Journal of Refrigeration*, 33(3): 635–644.
- Goodman, C., Fronk, B. M., and Garimella, S. (2011).** “Transcritical carbon dioxide microchannel heat pump water heaters: Part

- II – System simulation and optimization.” *International Journal of Refrigeration*, 34(4): 870–880.
- Halozan, H. (1997).** “Residential heat pump systems and controls.” *IEA Heat Pump Centre Newsletter*, 15(2): 19–21.
- Hamilton, J. and Miller, J. (1990).** “A Simulation Program for Modeling an Air-Conditioning System.” In “ASHRAE Transactions,” volume 96(1), pages 213–221. ASHRAE, Atlanta, United States.
- Jin, H. (2002).** *Parameter estimation based models of water source heat pumps*. Ph.d. thesis, Oklahoma State University.
- Karlsson, F. (2007).** *Capacity Control of Residential Heat Pump Heating Systems*. Ph.d. thesis, Chalmers University of Technology.
- Kim, M.-H., Pettersen, J., and Bullard, C. W. (2004).** “Fundamental process and system design issues in CO<sub>2</sub> vapor compression systems.” *Progress in Energy and Combustion Science*, 30(2): 119–174.
- Lemmon, E., Huber, M., and McLinden, M. (2007).** “NIST Standard Reference Database 23: Reference Fluid Thermodynamic and Transport Properties (REFPROP).”
- Liao, S. M., Zhao, T. S., and Jakobsen, A. (2000).** “A correlation of optimal heat rejection pressures in transcritical carbon dioxide cycles.” *Applied Thermal Engineering*, 20(9): 831–841.
- Lorentzen, G. (1994).** “Revival of carbon dioxide as a refrigerant.” *International Journal of Refrigeration*, 17(5): 292–301.
- Moran, M. J. and Shapiro, H. N. (2006).** *Fundamentals of Engineering Thermodynamics*. Wiley, 5th edition.
- Murugappan, A. (2002).** *Implementing ground source heat pump and ground loop heat exchanger models in the EnergyPlus simulation environment*. M.sc. thesis, Oklahoma State University.
- Nekså, P., Rekstad, H., Zakeri, G. R., et al. (1998).** “CO<sub>2</sub>-heat pump water heater: characteristics, system design and experimental results.” *International Journal of Refrigeration*, 21(3): 172–179.

- Novakovic, V., Bolland, O., Ulseth, R., et al. (2008).** *Kompendium TEP4225 Energi og Miljø.*
- NS3700 (2010).** “Criteria for passive houses and low energy buildings - Residential buildings.” Norsk Standard NS3700:2010, Standard Norge.
- Qi, P.-C., He, Y.-L., Wang, X.-L., et al. (2013).** “Experimental investigation of the optimal heat rejection pressure for a transcritical CO<sub>2</sub> heat pump water heater.” *Applied Thermal Engineering*, 56(1–2): 120–125.
- Robinson, D. M. and Groll, E. A. (1998).** “Efficiencies of transcritical CO<sub>2</sub> cycles with and without an expansion turbine: Rendement de cycles transcritiques au CO<sub>2</sub> avec et sans turbine d’expansion.” *International Journal of Refrigeration*, 21(7): 577–589.
- Rohsenow, W., Hartnett, J., and Cho, Y. (1998).** *Handbook of Heat Transfer.* McGraw-Hill, 3rd edition.
- Sarkar, J., Bhattacharyya, S., and Gopal, M. R. (2004).** “Optimization of a transcritical CO<sub>2</sub> heat pump cycle for simultaneous cooling and heating applications.” *International Journal of Refrigeration*, 27(8): 830–838.
- Sarkar, J., Bhattacharyya, S., and Gopal, M. R. (2006).** “Simulation of a transcritical CO<sub>2</sub> heat pump cycle for simultaneous cooling and heating applications.” *International Journal of Refrigeration*, 29(5): 735–743.
- Sarkar, J., Bhattacharyya, S., and Ram Gopal, M. (2005).** “Transcritical CO<sub>2</sub> heat pump systems: exergy analysis including heat transfer and fluid flow effects.” *Energy Conversion and Management*, 46(13–14): 2053–2067.
- Span, R. and Wagner, W. (1996).** “A New Equation of State for Carbon Dioxide Covering the Fluid Region from the Triple Point Temperature to 1100 K at Pressures up to 800 MPa.” *Journal of Physical and Chemical Reference Data*, 25(6): 1509–1596.
- Stene, J. (2004).** *Residential CO<sub>2</sub> Heat Pump System for Combined Space Heating and Hot Water Heating.* Ph.d. thesis, NTNU.

- Stene, J. (2009).** “Master Module 5: CO<sub>2</sub> Heat Pumps.” In “Natural Refrigerant CO<sub>2</sub>,” pages 225–291. KHLim.
- Stene, J. (2012a).** “Carbon Dioxide (R744) as a Working Fluid in Heat Pumps.” Class lecture, TEP16 "Heat Pump Technology". NTNU, Trondheim, Norway.
- Stene, J. (2012b).** “Dimensioning of Heat Pumps in Buildings.” Class lecture, TEP4260 "Heat Pumps for Heating and Cooling of Buildings". NTNU, Trondheim, Norway.
- Stene, J. and Skiple, T. (2007).** “Hybrid boligvarmesystem med termisk solfanger og CO<sub>2</sub>-luft/vann-varmepumpe.” Technical Report TR F6565, SINTEF Energiforskning AS, Trondheim.
- Uhlmann, M. and Bertsch, S. S. (2012).** “Theoretical and experimental investigation of startup and shutdown behavior of residential heat pumps.” *International Journal of Refrigeration*, 35(8): 2138–2149.
- Xu, X.-x., Chen, G.-m., Tang, L.-m., et al. (2011).** “Experimental evaluation of the effect of an internal heat exchanger on a transcritical CO<sub>2</sub> ejector system.” *Journal of Zhejiang University SCIENCE A*, 12(2): 146–153.
- Yamaguchi, S., Kato, D., Saito, K., et al. (2011).** “Development and validation of static simulation model for CO<sub>2</sub> heat pump.” *International Journal of Heat and Mass Transfer*, 54(9–10): 1896–1906.
- Yang, J. L., Ma, Y. T., Li, M. X., et al. (2005).** “Exergy analysis of transcritical carbon dioxide refrigeration cycle with an expander.” *Energy*, 30(7): 1162–1175.
- Yokoyama, R., Shimizu, T., Ito, K., et al. (2007).** “Influence of ambient temperatures on performance of a CO<sub>2</sub> heat pump water heating system.” *Energy*, 32(4): 388–398.

## Computer software

**CoolPack** (Technical University of Denmark) Heating/refrigeration cycle analysis and utilities. <http://www.ipu.dk/English/IPU-Manufacturing/Refrigeration-and-energy-technology/Downloads/CoolPack.aspx>

**EnergyPlus** (U.S. Department of Energy) Building energy simulation software. <http://apps1.eere.energy.gov/buildings/energyplus/>

**FluidProp** (TU Delft) Software w/Excel add-in for calculation of thermophysical properties of fluids. <http://fluidprop.tudelft.nl/>

**RefProp** (NIST) Reference fluid thermodynamic and transport properties database. <http://www.nist.gov/srd/nist23.cfm>

**Simply Fortran** (Approximatrix) Fortran editor, compiler and debugger. <http://simplyfortran.com/>

**SketchUp** (Trimble) 3D modelling software. <http://www.sketchup.com/>





# Appendices

## Appendix A List of digital attachments

- `Air-to-water.idf`: Example of EnergyPlus input file used for simulations.
- `Energy+.idd`: Edited version of the EnergyPlus Input Data Dictionary, defines the input syntax for the EnergyPlus input file objects.
- `EnergyPlus.exe`: EnergyPlus 7.1 program compiled from the edited source code.
- `EPlusSource` folder: Contains the edited modules of the EnergyPlus 7.1 source code. Most of the edits are minor edits made to the existing code in order for the heat pump model to work, except for the `PlantWaterToWaterGSHP.f90` which contains the implementation of the transcritical heat pump model described in Chapter 4.1 as part of the `CalcGshpModel` subroutine. Note that the rest of the unedited modules which can be obtained from the EnergyPlus website are also needed in order to compile and run the software.
  - `DataPlant.f90`
  - `FluidProperties.f90`
  - `PlantFluidCoolers.f90`
  - `PlantManager.f90`
  - `PlantPlateHeatExchanger.f90`
  - `PlantWaterToWaterGSHP.f90`
- `HPModel.xlsx`: MS Excel implementation of the heat pump model used for testing and preliminary study.
- `R744Properties.xlsx`: Saturated and superheated properties of CO<sub>2</sub> calculated from Span and Wagner (1996).
- `R744Properties.txt`: Same as `R744Properties.xlsx`, but converted into EnergyPlus input format.

## Appendix B COP vs. gas cooler UA-value

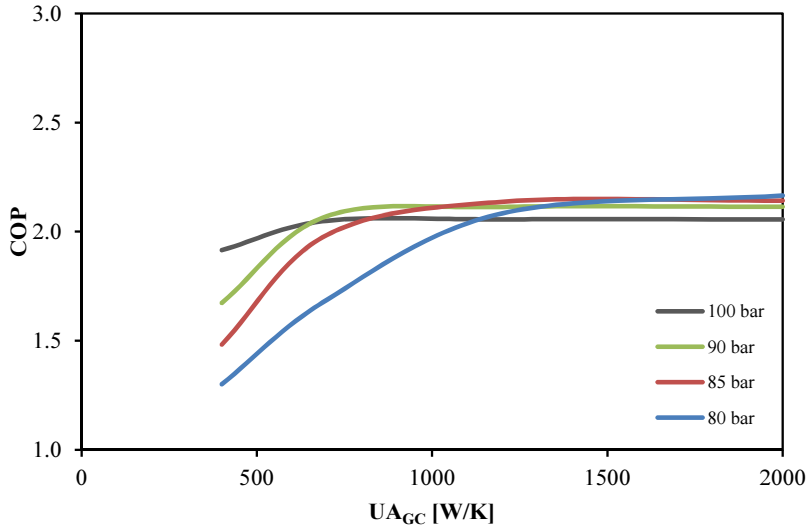


Figure B.1: COP vs. gas cooler UA-value at different gas cooler pressures. Secondary fluid heated from 30 to 35°C, evaporator UA-value is 400 W/K.

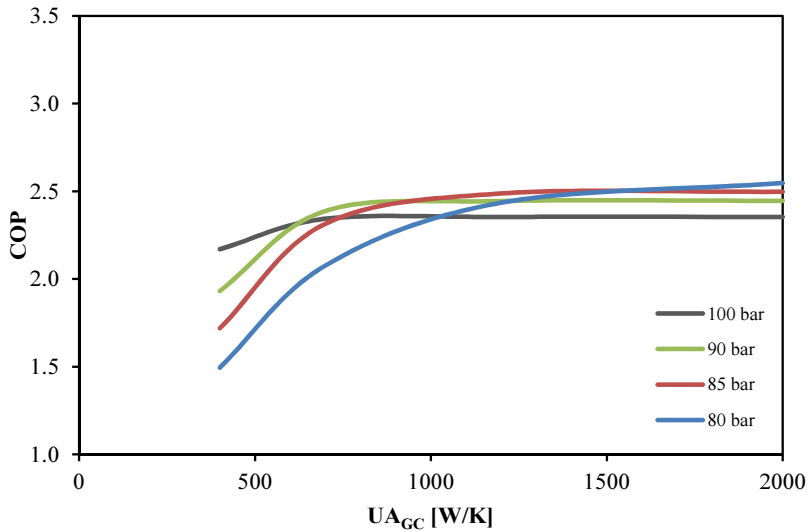


Figure B.2: COP vs. gas cooler UA-value at different gas cooler pressures. Secondary fluid heated from 7 to 65°C, evaporator UA-value is 400 W/K.

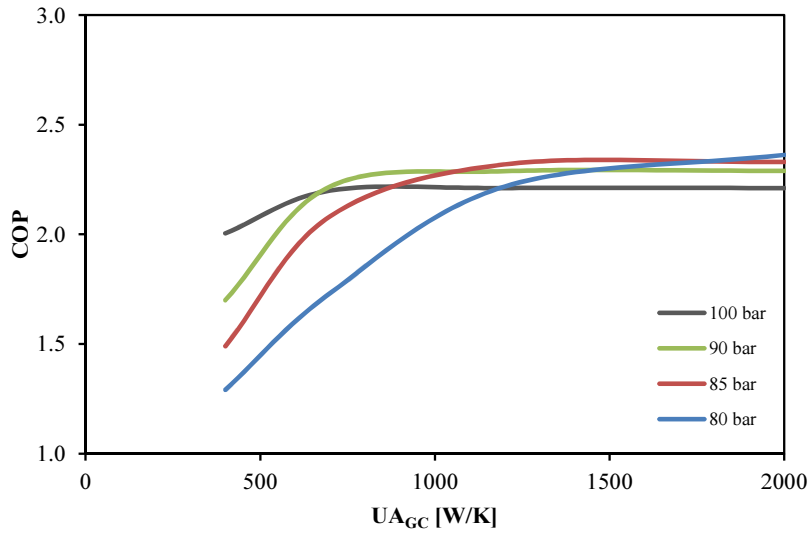


Figure B.3: *COP vs. gas cooler UA-value at different gas cooler pressures. Secondary fluid heated from 30 to 35°C, evaporator UA-value is 700 W/K.*

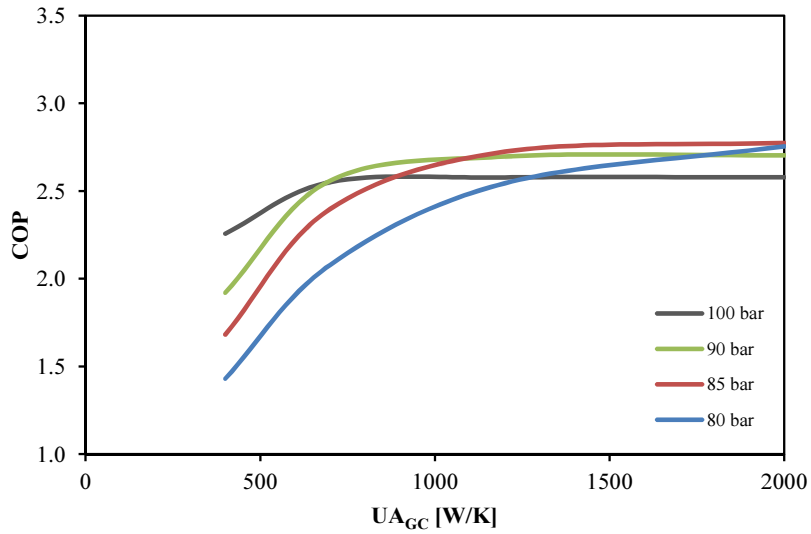


Figure B.4: *COP vs. gas cooler UA-value at different gas cooler pressures. Secondary fluid heated from 7 to 65°C, evaporator UA-value is 700 W/K.*

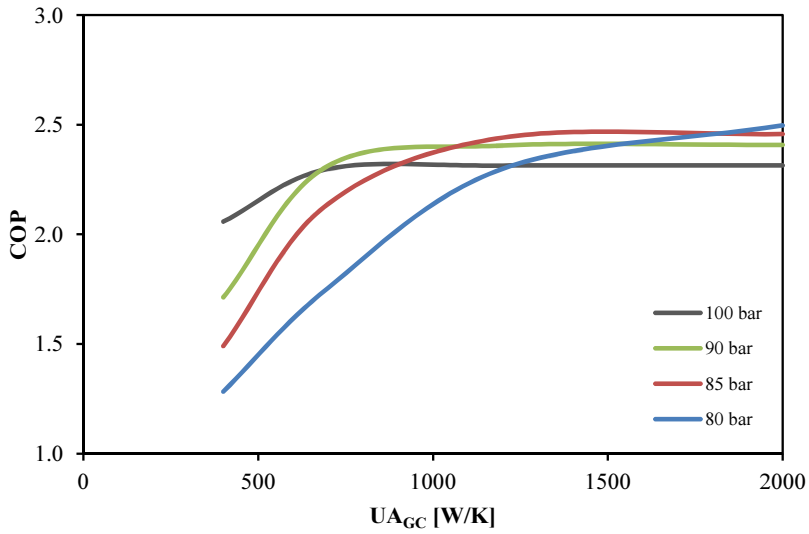


Figure B.5: COP vs. gas cooler UA-value at different gas cooler pressures. Secondary fluid heated from 30 to 35°C, evaporator UA-value is 1200 W/K.

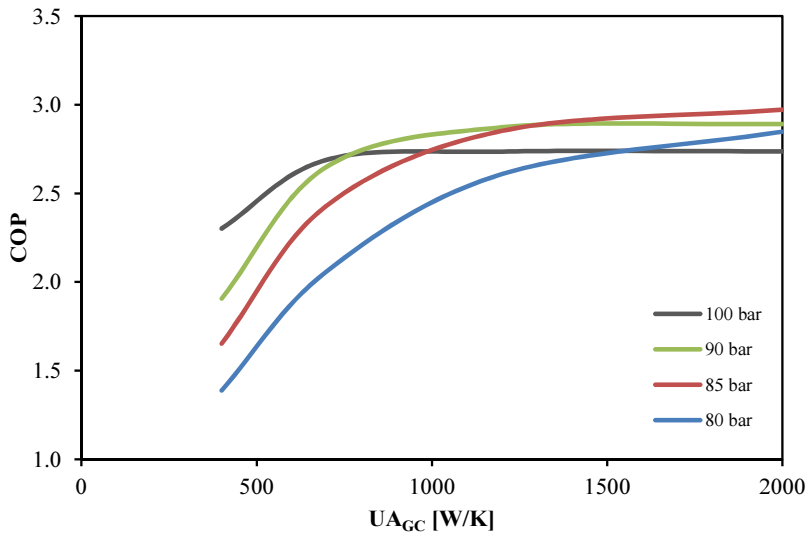


Figure B.6: COP vs. gas cooler UA-value at different gas cooler pressures. Secondary fluid heated from 7 to 65°C, evaporator UA-value is 1200 W/K.

## Appendix C Optimal gas cooler pressure curves

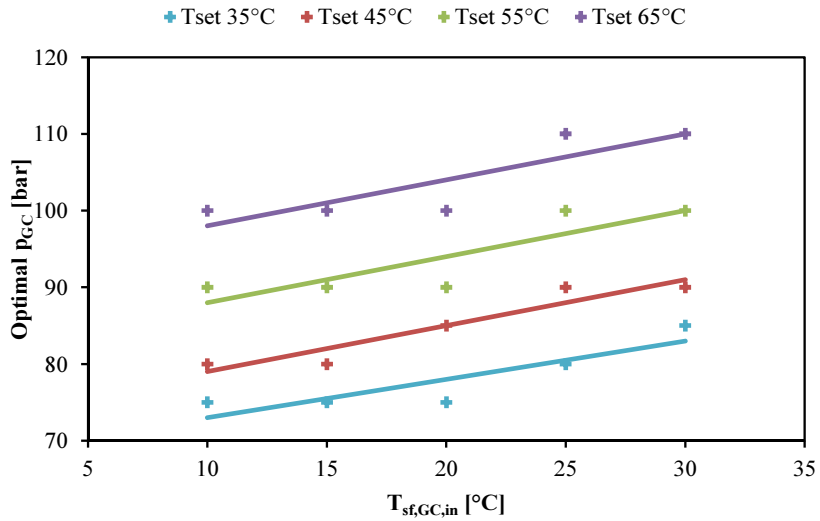


Figure C.1: Least-squares curve-fit of optimal gas cooler pressure variation with secondary fluid inlet temperature (Equation 4.13, Chapter 4.3)

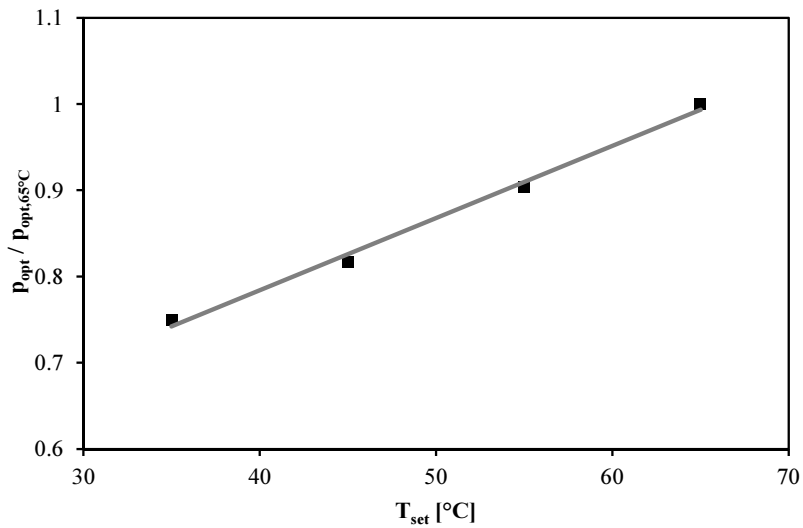


Figure C.2: Least-squares curve-fit of optimal gas cooler pressure variation with secondary fluid setpoint temperature (Equation 4.13, Chapter 4.3)

## Appendix D Heat pump model source code

**Description:** Fortran90 source code for the transcritical heat pump model described in Chapter 4.1 and implemented into EnergyPlus. This is part of the CalcGshpModel subroutine in the PlantWaterToWaterGSHP.f90 module.

```
! Starting heat pump calculations
! Heat transfer rates initial guess
initialQSource = 0.0
initialQLoad   = 0.0
IterationCount = 0

! Determine evaporator effectiveness
SourceSideEffect = 1- EXP( -SourceSideUA / &
                          (CpWaterSourceSide * SourceSideWaterMassFlowRate))

LOOPLoadEnth: DO ! Main loop
  IterationCount = IterationCount+1

  ! Determine evaporator temperature (if above critical point, set to below -
  ! if below lower limit, set to limit)
  SourceSideTemp = SourceSideWaterInletTemp - initialQSource/ &
                  (SourceSideEffect * CpWaterSourceSide * &
                  SourceSideWaterMassFlowRate)

  IF (SourceSideTemp > 30.9) THEN
    SourceSideTemp = 30.9
  END IF
  IF (SourceSideTemp < -40.0) THEN
    SourceSideTemp = -40.0
  END IF

  ! Determine evaporator and gas cooler pressure
  SourceSidePressure = GetSatPressureRefrig(GSHPRefrigerant,SourceSideTemp, &
      GSHPRefrigIndex,'CalcGSHPModel:SourceSideTemp')
  LoadSidePressure = ((0.00504 * SetpSchedValue * LoadSideWaterInletTemp) + &
      (0.773 * SetpSchedValue) + (0.269 * LoadSideWaterInletTemp) &
      + 41.3) * 100000.0

  ! Check upper/lower pressure limit 120 bar/75 bar
  IF (LoadSidePressure > 12000000.0) THEN
    LoadSidePressure = 12000000.0
  ELSE IF (LoadSidePressure < 7500000.0) THEN
    LoadSidePressure = 7500000.0
  END IF

  ! Check if outside pressure limits
  IF (SourceSidePressure < LowPressCutOff) THEN
    CALL ShowSevereError(ModuleCompName//=''//trim(GSHPName)//'' Heating &
      Source Side Pressure Less than the Design Minimum')
```

```

CALL ShowContinueError('Source Side Pressure='//TRIM(TrimSigDigits( &
    SourceSidePressure,2))//') and user specified Design &
    Minimum Pressure='//TRIM(TrimSigDigits(LowPressCutoff,2)))
CALL ShowFatalError('Preceding Conditions cause termination.')
END IF
IF (LoadSidePressure > HighPressCutOff) THEN
CALL ShowSevereError(ModuleCompName//'"//trim(GSHpname)//'" Heating &
    Load Side Pressure greater than the Design Maximum')
CALL ShowContinueError('Load Side Pressure='//TRIM(TrimSigDigits( &
    LoadSidePressure,2))//') and user specified Design &
    Maximum Pressure='//TRIM(TrimSigDigits(HighPressCutOff,2)))
CALL ShowFatalError('Preceding Conditions cause termination.')
END IF

! Determine compressor suction and discharge pressure
SuctionPr = SourceSidePressure - PressureDrop
DischargePr = LoadSidePressure

! Check if outside pressure limits
IF (SuctionPr < LowPressCutOff) THEN
CALL ShowSevereError(ModuleCompName//'"//trim(GSHpname)//'" Heating &
    Suction Pressure Less than the Design Minimum')
CALL ShowContinueError('Heating Suction Pressure='//TRIM(TrimSigDigits( &
    SuctionPr,2))//') and user specified Design Minimum &
    Pressure='//TRIM(TrimSigDigits(LowPressCutoff,2)))
CALL ShowFatalError('Preceding Conditions cause termination.')
END IF
IF (DischargePr > HighPressCutOff) THEN
CALL ShowSevereError(ModuleCompName//'"//trim(GSHpname)//'" Heating &
    Discharge Pressure greater than the Design Maximum')
CALL ShowContinueError('Heating Discharge Pressure='//TRIM(TrimSigDigits( &
    DischargePr,2))//') and user specified Design Maximum &
    Pressure='//TRIM(TrimSigDigits(HighPressCutOff,2)))
CALL ShowFatalError('Preceding Conditions cause termination.')
END IF

! Determine evaporator outlet enthalpy
qual=1.0
SourceSideOutletEnth = GetSatEnthalpyRefrig(GSHPrefrigerant, SourceSideTemp, &
    qual,GSHPrefrigIndex,'CalcGSHPMODEL:SourceSideTemp')

! Determine superheat temperature
CompSuctionTemp = SourceSideTemp + ShTemp

! Determine superheated enthalpy
CompSuctionEnth = GetSupHeatEnthalpyRefrig(GSHPrefrigerant,CompSuctionTemp, &
    SuctionPr,GSHPrefrigIndex,'CalcGSHPMODEL:CompSuctionTemp')
IF (CompSuctionEnth < SourceSideOutletEnth) THEN
! In case interpolation falls out of superheated region
CompSuctionTemp = SourceSideTemp
CompSuctionEnth = SourceSideOutletEnth
ENDIF

```

```

! Determine refrigerant mass flow rate
CompSuctionDensity = GetSupHeatDensityRefrig(GSHPrefrigerant, CompSuctionTemp, &
      SuctionPr,GSHPrefrigIndex,'CalcGSHPModel:CompSuctionTemp')
MassRef = VolEfficiency * CompSuctionDensity * PistonDisp

! Determine compressor ISENTROPIC discharge temperature and enthalpy
qual = 1.0
SourceSideOutletEntr = GetSatEntropyRefrig(GSHPrefrigerant, SourceSideTemp, &
      qual,GSHPrefrigIndex,'CalcGSHPModel:CompSuctionTemp')
CompSuctionEntropy = GetSupHeatEntropyRefrig(GSHPrefrigerant, CompSuctionTemp, &
      SuctionPr,GSHPrefrigIndex,'CalcGSHPModel:CompSuctionTemp')
IF (CompSuctionEntropy < SourceSideOutletEntr) THEN
  ! In case interpolation falls out of superheated region
  CompSuctionEntropy = SourceSideOutletEntr
ENDIF

CompDischargeTemp = GetSupHeatTempEntropyRefrig(GSHPrefrigerant, CompSuctionEntropy, &
      DischargePr,GSHPrefrigIndex,'CalcGSHPModel:CompSuctionEntropy')
LoadSideInletEnth = GetSupHeatEnthalpyRefrig(GSHPrefrigerant, CompDischargeTemp, &
      DischargePr,GSHPrefrigIndex,'CalcGSHPModel:CompDischargeTemp')

! Determine compressor ACTUAL discharge enthalpy and temperature
LoadSideInletEnth = CompSuctionEnth + ((LoadSideInletEnth - CompSuctionEnth) / &
      IsenEfficiency) * (1.d0 - CompHeatLossFactor)
CompDischargeTemp = GetSupHeatTempEnthalpyRefrig(GSHPrefrigerant, LoadSideInletEnth, &
      DischargePr,GSHPrefrigIndex,'CalcGSHPModel:LoadSideInletEnth')

! Determine gas cooler CO2 inlet temperature
LoadSideInletTemp = GetSupHeatTempEnthalpyRefrig(GSHPrefrigerant, LoadSideInletEnth, &
      LoadSidePressure,GSHPrefrigIndex,'CalcGSHPModel:LoadSideInletEnth')

! Determine compressor power
Power = (1.0 / (1.0 - CompHeatLossFactor)) * MassRef * &
      (LoadSideInletEnth - CompSuctionEnth)

! Guess initial linear temperature profile
SubSecWaterInletTemp(0) = LoadSideWaterInletTemp
LOOPGasCoolerInit: DO i = 0,NumberOfSubsections
  SubSecRefrigInletTemp(i) = LoadSideInletTemp - (((NumberOfSubsections - i) / &
      NumberOfSubsections) * (LoadSideInletTemp - LoadSideWaterInletTemp))
END DO LOOPGasCoolerInit

! Initialize gas cooler loop
SubSectionUA = LoadSideUA / NumberOfSubsections
GasCoolerDidConverge = .FALSE.
IterationCountGC = 0

LOOPGasCooler: DO ! Main gas cooler loop
  IterationCountGC = IterationCountGC + 1

  ! Reset variables before each iteration
  SubsecError = 0.d0
  RefrigSideTotHeat = 0.d0

```



```

WaterSideTotHeat = 0.d0
LoadSideOutletTemp = SubSecRefrigInletTemp(0)

! Loop through all subsections, determine properties and heat transfer
! balance within each subsection
LOOPSubSections: DO i = 1,NumberOfSubsections ! Gas cooler subsections loop
  AvgTemp = SubSecRefrigInletTemp(i-1) + (SubSecRefrigInletTemp(i) - &
    SubSecRefrigInletTemp(i-1)) / 2
  CpRefrig = GetSupHeatSpecificHeatRefrig(GSHPRRefrigerant, AvgTemp, &
    LoadSidePressure,GSHPRRefrigIndex,'CalcGSHPModel:AvgTemp')

  ! Determine minimum heat capacity
  IF ((MassRef * CpRefrig) < (LoadSideWaterMassFlowRate * CpWaterLoadSide)) THEN
    CMin = MassRef * CpRefrig
    CRel = CMin / (LoadSideWaterMassFlowRate * CpWaterLoadSide)
  ELSE
    CMin = LoadSideWaterMassFlowRate * CpWaterLoadSide
    CRel = CMin / (MassRef * CpRefrig)
  END IF

  ! Determine number of transfer units
  NTU = SubSectionUA / CMin

  ! Determine heat exchanger effectiveness
  IF (CRel <= 0.9) THEN
    Eff = (1.d0 - EXP(-NTU*(1.d0-CRel))) / (1.d0 - CRel*EXP(-NTU*(1.d0-CRel)))
  ELSE
    Eff = NTU / (1.d0 + NTU)
  END IF

  ! Determine heat transfer rates to/from water and refrigerant
  SubSecHeat(i) = Eff * CMin * (SubSecRefrigInletTemp(i) - &
    SubSecWaterInletTemp(i-1))
  SubSecRefrigHeat(i) = MassRef * CpRefrig * (SubSecRefrigInletTemp(i) - &
    SubSecRefrigInletTemp(i-1))

  ! Add subsection heat transfer rate to total rates
  WaterSideTotHeat = WaterSideTotHeat + SubSecHeat(i)
  RefrigSideTotHeat = RefrigSideTotHeat + SubSecRefrigHeat(i)

  ! Calculate the error based on the heat transfer rate balance -
  ! set it as error value if higher than the current highest
  IF (ABS((SubSecHeat(i) - SubSecRefrigHeat(i)) / &
    (SubSecRefrigHeat(i) + SmallNum)) > SubsecError) THEN
    SubsecError = ABS((SubSecHeat(i) - SubSecRefrigHeat(i)) / &
    (SubSecRefrigHeat(i) + SmallNum))
  END IF

  ! Set inlet water temperature for next subsection
  SubSecWaterInletTemp(i) = SubSecWaterInletTemp(i-1) + (SubSecHeat(i) / &
    (LoadSideWaterMassFlowRate * CpWaterLoadSide))

  ! Estimate new refrigerant inlet temperature (for next gas cooler iteration)

```

```

        SubSecRefrigInletTemp(i-1) = SubSecRefrigInletTemp(i) - (SubSecHeat(i) / &
            (MassRef * CpRefrig))
    END DO LOOPSubSections

    ! Exit the loop if satisfying convergence or passed iteration limit
    IF (SubSecError < HeatBalTolGC) THEN
        GasCoolerDidConverge = .TRUE.
        EXIT LOOPGasCooler
    ELSE IF (IterationCountGC > IterationLimitGC) THEN
        EXIT LOOPGasCooler
    END IF
END DO LOOPGasCooler

! Determine the gas cooler outlet enthalpy (and evaporator inlet enthalpy
! for an isenthalpic expansion)
LoadSideOutletEnth = GetSupHeatEnthalpyRefrig(GSHPrefrigerant,LoadSideOutletTemp, &
    LoadSidePressure,GSHPrefrigIndex,'CalcGSHPMoel:LoadSideOutletTemp')

! Determine evaporator heat transfer rate
QSource = MassRef * (SourceSideOutletEnth - LoadSideOutletEnth)

! Determine gas cooler heat transfer rate and water mass flow rate
QLoad = ((1.0 - CompHeatLossFactor) / 1.0) * Power + QSource
LoadSideWaterMassFlowRate = QLoad / (CpWaterLoadSide * (SetpSchedValue - &
    LoadSideWaterInletTemp))

ErrQLoad    = ABS((QLoad - initialQLoad)/(initialQLoad+SmallNum))
ErrQSource  = ABS((QSource - initialQSource)/(initialQSource+SmallNum))

! Exit the loop if satisfying convergence or passed iteration limit
IF((ErrQLoad<HeatBalTol .AND. ErrQSource<HeatBalTol) .OR. &
    IterationCount>IterationLimit) THEN
    IF(IterationCount>IterationLimit) THEN
        CALL ShowWarningError(ModuleCompName//' did not converge')
        CALL ShowContinueErrorTimeStamp(' ')
        CALL ShowContinueError('Heatpump Name = '//TRIM(GSHP(GSHPNuM)%Name))
        ! Note 16.04: Must be changed to MODULE variables!
        IF (.NOT. GasCoolerDidConverge) THEN
            CALL ShowWarningError(ModuleCompName//' GAS COOLER did not converge')
            CALL ShowContinueErrorTimeStamp(' ')
            CALL ShowContinueError('Heatpump Name = '//TRIM(GSHP(GSHPNuM)%Name))
            WRITE(ErrString,*) ABS(100.0 * SubSecError)
            CALL ShowContinueError('Max. Subsection Heat Inbalance (%) = &
                '//TRIM(ADJUSTL(ErrString)))
            WRITE(ErrString,*) WaterSideTotHeat
            CALL ShowContinueError('Water-side heat transfer rate      = &
                '//TRIM(ADJUSTL(ErrString)))
            WRITE(ErrString,*) RefrigSideTotHeat
            CALL ShowContinueError('Refrigerant-side heat transfer rate = &
                '//TRIM(ADJUSTL(ErrString)))
            WRITE(ErrString,*) SubSecWaterInletTemp(0)
            CALL ShowContinueError('Water inlet temperature          = &
                '//TRIM(ADJUSTL(ErrString)))
        END IF
    END IF
END IF

```

```

        WRITE(ErrString,*) SubSecRefrigInletTemp(NumberOfSubsections)
        CALL ShowContinueError('Refrigerant inlet temperature      = &
        '//TRIM(ADJUSTL(ErrString)))
    END IF
END IF
EXIT LOOPLoadEnth

ELSE ! Update heat transfer rates with new guess
    initialQLoad = initialQload + RelaxParam*(QLoad - initialQLoad)
    initialQSource = initialQSource + RelaxParam*(QSource - initialQSource)
END IF

END DO LOOPLoadEnth

GasCoolerInletTemp    = LoadSideInletTemp
GasCoolerOutletTemp  = LoadSideOutletTemp
GasCoolerPressure     = LoadSidePressure
EvaporatorTemp       = SourceSideTemp

! Heat pump load
IF(ABS(MyLoad) < QLoad) THEN
    DutyFactor = ABS(MyLoad)/QLoad
    QLoad = ABS(MyLoad)
    Power = DutyFactor * Power
    QSource = QSource * DutyFactor
    LoadSideWaterMassFlowRate = DutyFactor * LoadSideWaterMassFlowRate
END IF

! Update temperatures, set load side flow rate
LoadSideWaterOutletTemp = LoadSideWaterInletTemp + QLoad/ &
    (LoadSideWaterMassFlowRate * CpWaterLoadSide)
SourceSideWaterOutletTemp = SourceSideWaterInletTemp - QSource/ &
    (SourceSideWaterMassFlowRate * CpWaterSourceSide)
CALL SetComponentFlowRate(LoadSideWaterMassFlowRate,LoadSideInletNode, &
    LoadSideOutletNode,GSHP(GSHPNum)%LoadLoopNum, &
    GSHP(GSHPNum)%LoadLoopSideNum,GSHP(GSHPNum)%LoadBranchNum, &
    GSHP(GSHPNum)%LoadCompNum)

! Setup report variables
GshpReport(GSHPNum)%WasOn = 1
GshpReport(GSHPNum)%GasCoolerInletTemp = GasCoolerInletTemp
GshpReport(GSHPNum)%GasCoolerOutletTemp = GasCoolerOutletTemp
GshpReport(GSHPNum)%GasCoolerPressure = GasCoolerPressure
GshpReport(GSHPNum)%EvaporatorTemp = EvaporatorTemp

RETURN

```

